NEXT-GENERATION ANALYTICAL SOLUTIONS FOR CELL & GENE THERAPY

YOU HELP PATIENTS. WE WILL HELP YOU GET THERE.

bio-techne®

Cell & Gene Therapies (C&GT) are a promising, rapidly growing area of research, and ProteinSimple is here to help you get safe and effective treatments to the people who need them. ProteinSimple's analytical platforms give you the automation and scalability needed for the development and manufacturing of C&GT products, and with low volume requirements, we help you preserve these precious samples. Platform methods can be seamlessly transferred across labs and project phases, from discovery to manufacturing, giving you consistent results from start to finish.

- **Automation:** Automated sample handling and processing give you more consistent, high-quality data.
- **Scalability:** Our platforms easily fit into your current workflows and adapt to your changing needs. No matter what throughput you need, results will be robust and reproducible whether you're scaling up or scaling out.
- **Method Transferability:** Seamlessly transfer analytical methods between labs and across phases from discovery to manufacturing with complete confidence in your method performance and regulatory compliance.
- **Low Sample Volumes:** With minimum sample volumes as low as 3 µL, our platforms can get you the data you need using as little of your precious sample as possible.

ANALYTICAL SOLUTIONS FOR CELL & GENE THERAPY

Maurice is the next generation icIEF and CE-SDS instrument that enables you to determine the stability, identity, and purity of your AAV vectors and LNPs with absorbance and fluorescence detection. Maurice also enables assessment of empty versus full AAV capsids.

Maurice

Simple Western automates traditional Western blotting while maximizing multiplexing with multiple detection channels. Use Simple Western for vector characterization and purity assessment in addition to monitoring your AAV capsid during purification. You can also use Simple Western for bioprocess contaminant detection.

Simple Western

Milo is the world's first automated Single-Cell Western platform, measuring protein expression in approximately 1000 single cells per run. Use Milo to measure gene editing efficiency and expression at a single-cell resolution.

Milo

Simple Plex assays on Ella provide rapid automated immunoassay with a high level of throughput, reproducibility, and ease of assay transfer to enable faster process decisions. Profile cytokines, measure viral titre, process impurities, and rapidly characterize cell expansion & functionality with parallel multianalyte analysis from the same sample.

Ella

Micro-Flow Imaging (MFI) directly images, counts, and characterizes subvisible particles like AAV and lentivirus aggregates and contaminants, and MFI monitors the impact of ultra-filtration on vector preparations. MFI can also detect residual beads used for activation in CAR T-cell therapy products.

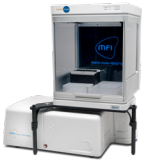

MFI

CONTENTS

CHAPTER 1: icIEF ANALYSIS OF ADENO-ASSOCIATED VIRUS (AAV) PROTEINS FOR GENE THERAPY

INTRODUCTION

In medicine, gene therapy is the process where nucleic acids are delivered to a patient's cells as a therapeutic drug to treat genetic diseases including hematological, immunological, neurodegenerative, and metabolic disorders, as well as several types of cancers. Once in the nucleus, the therapeutic DNA or RNA replaces a mutant gene with a functional gene, knocks-out a mutated gene that is functioning incorrectly, or introduces a new gene into the body to help fight disease. Moreover, the development of versatile gene-editing technologies like CRISPR, which make it faster and more reliable to modify target DNA, elevates the promise gene therapy holds as a potential treatment option.

All gene therapies utilize either viral or non-viral vectors to deliver the DNA or RNA into the host cell. Viral vectors infect the host cell to introduce the genetic material and are more efficient at transfecting the host cell compared to non-viral vectors like cationic lipids or chemical carriers. However, they can have immunogenic side effects depending on the specific virus used. Therefore, the choice of appropriate viral vector is a critical component when developing the drug. Adeno-associated virus (AAV) is non-pathogenic, and thus incurs only minimal immune response, making it an ideal gene therapy vector.

As with all therapeutic drugs, product characterization is of utmost importance in order to ensure drug safety and stability. For gene therapies, this includes characterizing the delivery vector before the drug is packaged. In this study, we demonstrate how imaged-capillary isoelectric focusing (icIEF) can be used to characterize the charge heterogeneity of AAV vectors to ensure product stability and identity. Maurice delivers this critical analysis as an automated platform that removes the variability typically encountered with platforms that require more hands-on time, and generates high-resolution data in less than 10 minutes. More importantly, Maurice offers 3-5x higher sensitivity than absorbance with the native fluorescence detection mode, offering significant advantages when characterizing low concentration AAV samples.

MATERIAL AND METHODS

REAGENTS

AAV2 (1 x 10^{13} GC/mL) and AAV6 (5 lots that ranged from 3.8 x 10^{12} – 8.5 x 10^{13} GC/mL) samples were obtained from Vigene Biosciences. The a la carte pI marker 9.46 was acquired from ProteinSimple (catalog #102349) while the SimpleSol Protein Solubilizer, methylcellulose, Pharmalyte 3-10 and 5-8, and the Maurice 5.85 and 8.40 pI markers were all obtained from the ProteinSimple Maurice cIEF Method Development Kit (catalog #PS-MDK01-C). Dithiothreitol (DTT) from TOCRIS (catalog #3154) was reconstituted using HPLC grade deionized water to a stock concentration of 80 mM. Dimethyl sulfoxide (DMSO) was purchased from Sigma (catalog #D2650-5x5ML) along with Formamide (catalog #F9037).

INTACT AAV ANALYSIS

AAV samples were analyzed with a method that does not disassociate assembled capsids, leaving them intact during focusing on Maurice. To prevent aggregation, the AAV samples were diluted 25-fold into a master mix, with the final prepared sample containing 50% SimpleSol, 0.35% methylcellulose, 4% 3–10 Pharmalyte, and Maurice pI markers 5.85 and 9.46. The intact AAV samples were run using a Maurice cIEF cartridge (catalog #PS-MC02-C) and pre-focused for 1 minute at 1,500 V then focused at 3,000 V for 7 minutes. Absorbance and native fluorescence images (20- and 80-seconds) were captured and analyzed using Compass for iCE software.

DENATURED AAV ANALYSIS

The AAV samples were denatured by heating the sample in the presence of 33% DMSO and 16.5 mM DTT for 10 minutes at 70 °C, then cooled to room temperature. Samples were then prepared for Maurice analysis by diluting the denatured sample 5-fold, with the final prepared sample containing 0.35% methylcellulose, 2% Pharmalyte 5–8 and 2% Pharmalyte 3–10, 40% formamide, and Maurice pI standards 5.85 and 8.40. Samples were separated using a Maurice cIEF cartridge (catalog #PS-MC02-C) for 1 minute at 1,500 V followed by 12 minutes at 3,000 V. Absorbance and native fluorescence images (20- and 80-seconds) were captured and analyzed using Compass for iCE software.

REPRODUCIBLE ANALYSIS OF INTACT AAV

We developed a method to analyze intact AAV particles on Maurice using native fluorescence to get a better understanding of the product as it pertains to particle stability and identity. We first assessed the intra-assay reproducibility of the intact AAV method on Maurice to determine whether Maurice could be used to reliably quantitate AAV samples.

When intact AAV2 and intact AAV6 (~3 x 10^{12} GC/mL) samples were examined on Maurice using absorbance and native fluorescence detection, a similar apparent pI for both serotypes around pI ~9.0 was observed (**FIGURE 1**). AAV2 appeared as a single peak, just below pI ~9.0 while the intact AAV6 sample resolved into 2 peaks and had an apparent pI ~9.25. A clear advantage of using fluorescence detection was observed as native fluorescence is 3–5x more sensitive compared to absorbance detection, which translates to higher signal-to-noise ratios. For example, the signal-to-noise for the AAV2 peak just below pI ~9.0 was 13.9 using absorbance detection and 36.2 with an 80-second exposure using native fluorescence detection. For AAV6, the peak using absorbance detection was very close to the baseline with a signal-to-noise of 2.9, bringing into question whether the peak can be reliably detected using absorbance. In comparison, the peak using native fluorescence using an 80-second exposure had a signal-to-noise of 24.1. This gain in sensitivity made it possible to save precious AAV sample since less starting material was required for analysis.

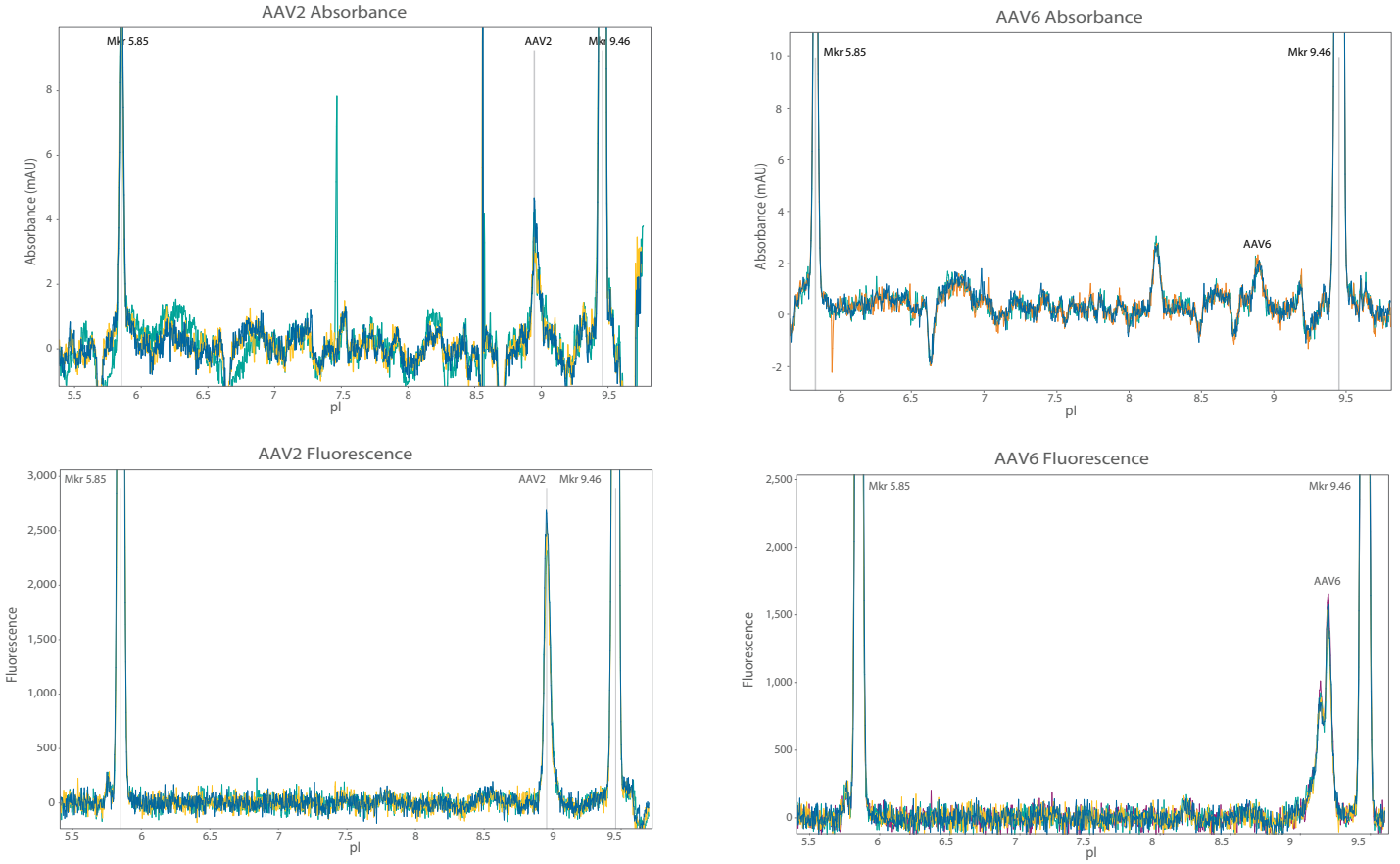

FIGURE 1. Apparent pI comparison of intact AAV2 and AAV6 particles. The intact AAV2 resolves as a single peak just below pI ~9.0 (left) while the intact AAV6 resolves as 2 peaks at an apparent pI ~9.25 (right). Native fluorescence detection (bottom) was clearly more sensitive compared to absorbance detection (top), making it possible to save precious sample when performing intact AAV analytics.

The intra-assay reproducibility of the intact method was then gauged by analyzing the total area for quadruplicate injections of the AAV2 and AAV6 samples (**FIGURE 2**). Results for both viral samples were very reproducible, with a %RSD of 3.95% and 4.30% for AAV2 and AAV6, respectively (**TABLE 1**).

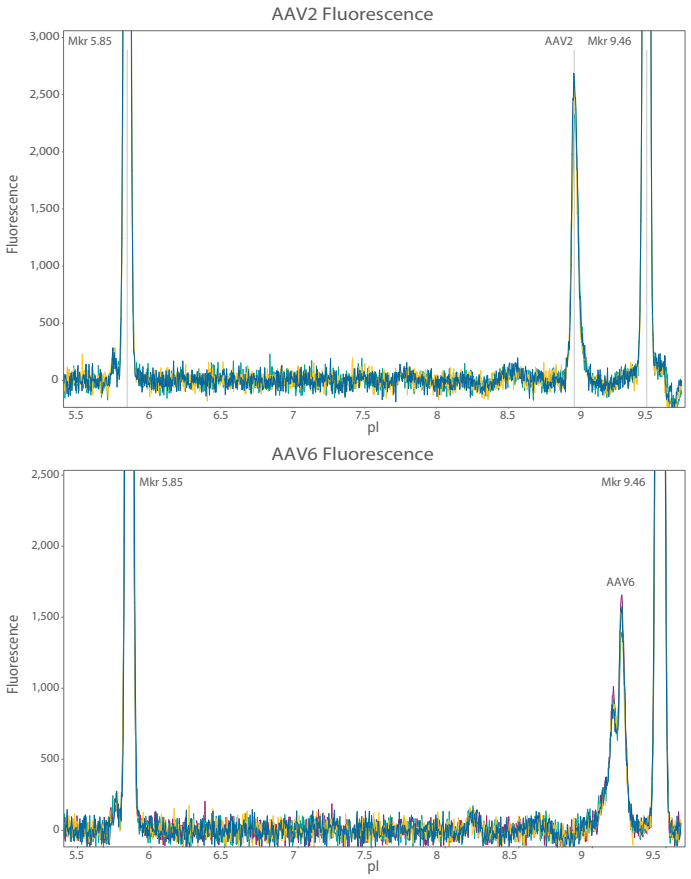

FIGURE 2. An overlay of quadruplicate injections of intact AAV2 (top) and AAV6 (bottom) visually demonstrates the intra-assay reproducibility of the intact AAV method. Fluorescence data are shown with 80-second exposures.

SAMPLE	INTACT AAV2 AREA	INTACT AAV6 AREA
Injection 1	47867	34711
Injection 2	43590	36932
Injection 3	47992	34636
Injection 4	46225	38318
Mean	1827.69	36149.25
%RSD	3.95	4.30

TABLE 1. Quantitative results from the quadruplicate injections of intact AAV2 and AAV6 demonstrates the intra-assay reproducibility of the intact AAV method. The results were very reproducible with %RSDs of 3.95% and 4.30% for the intact AAV2 and AAV6, respectively.

We then assessed the inter-assay reproducibility by running an AAV6 sample (~ 3 x 10^{12} GC/mL) in triplicate on three separate days, for a total of nine injections. Due to limited sample availability, only the intact AAV6 was used to evaluate the inter-assay reproducibility of the method (**FIGURE 3**). Quantitation of the total peak area suggests the method was highly reproducible, with a %RSDs of 6.6% (**TABLE 2**).

REPRODUCIBLE ANALYSIS OF DENATURED AAV

AAV viral proteins are subject to several post-translational modifications, including glycosylation and deamidation. Stress-induced deamidation of viral proteins can lead to a loss of vector activity, capsid assembly, and transduction efficiency[1].

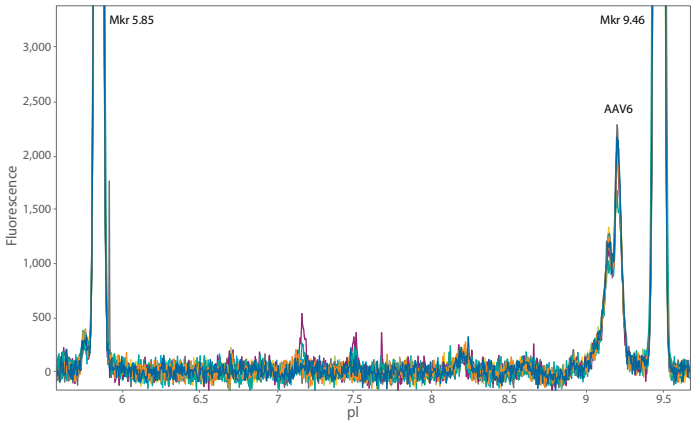

FIGURE 3. An overlay of nine injections, run over the course of three days, of intact AAV6 visually demonstrates the inter-assay reproducibility of the intact AAV method (data shown for 80 second fluorescence exposure).

	TOTAL PEAK AREA
Day 1	42245 49481 50006
Day 2	47217 48165 45943
Day 3	51304 51270 53871
Mean	48834
%RSD	6.60

TABLE 2. Quantitative results from nine injections, where samples were run in triplicate over three days, confirm the inter-assay reproducibility of the intact AAV method, with a %RSD of 6.60% for the total peak area.

Denatured icIEF methods are commonly utilized to monitor charge heterogeneity of monoclonal antibodies induced by sialylation, glycation, and deamidation, so we hypothesized similar assessments could be performed on AAV viral proteins.

To confirm that Maurice can be used to characterize the viral vector, we denatured AAV2 (~1 x 10^{12} GC/mL) prior to analysis and evaluated the reproducibility of the denatured AAV method. AAV2 charge variants were clearly resolved and reproducible when evaluated visually using an overlay of triplicate electropherograms using both absorbance and native fluorescence detection (**FIGURE 4**). Quantitation of the total peak area further confirms the intra-assay reproducibility of the data, as the % RSDs for the total area was 3.2% using absorbance detection and 1.5% using native fluorescence detection (**TABLE 3**). As with the intact AAV method, native fluorescence detection was more sensitive compared to absorbance detection, which translates to better baseline resolution and higher signal-to-noise ratios. A 10x increase was observed when assessing the minor peak at pI 6.5, as the signal-to-noise for absorbance and native fluorescence with an 80-second exposure was 2.1 and 23.6, respectively. Again, this results in significant sample savings, as less AAV starting material is required to perform icIEF analysis using fluorescence detection on Maurice.

The inter-assay reproducibility of denatured methods was also assessed using the AAV6 sample. The denatured AAV6 (~6 x 10^{12} GC/mL) was run in triplicate on three different days. The inter-assay performance was highly reproducible (**FIGURE 5**). The data quantitation confirmed this, as the peaks with greater than 10% average percent composition all had %RSDs under 7.5% for percent peak area, and the standard deviation for the pI values were all under 0.02 (**TABLE 4**).

MAURICE icIEF METHOD IS SENSITIVE AND LINEAR

To establish the method's sensitivity, we then serially titrated the denatured AAV2 from ~3 x 10^{12} GC/mL down to ~3 x 10^{11} GC/mL (**FIGURE 6**). A blank buffer was also included as a negative control. Maurice was able to detect AAV2 protein from a sample with as little as 3 x 10^{11} GC/mL using native fluorescence detection, with a calculated limit of detection of ~1 x 10^{11} GC/mL. A strong linear correlation was observed across this titration range, with an R^2 of 0.9956.

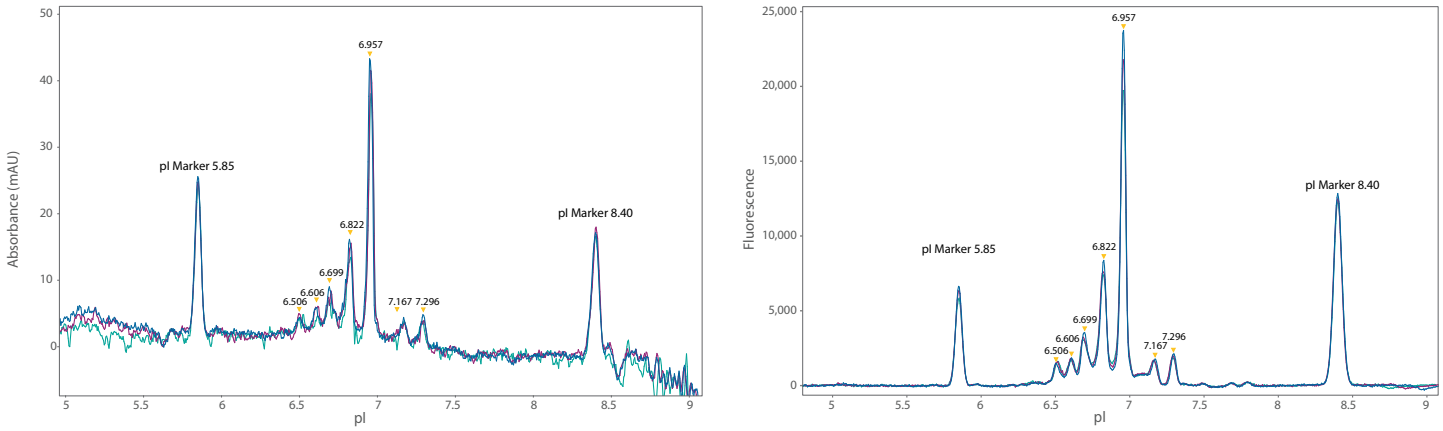

FIGURE 4. The denatured icIEF method for AAV2 is reproducible for both absorbance (left) and native fluorescence (right) detection within a run. Shown are overlays of three injections for both detection modes. Data generated with native fluorescence detection had improved signal-to-noise ratios and baseline resolution compared to absorbance detection.

INJECTION	TOTAL PEAK AREA (ABSORBANCE)	TOTAL PEAK AREA (NATIVE FLUORESCENCE)
1	926	488620
2	999	474643
3	985	491055
Mean	970	484773
%RSD	3.2	1.5

TABLE 3. Denatured AAV2 quantitation on Maurice is reproducible. %RSDs for the total peak area were 3.2% using UV absorbance detection and 1.5% using native fluorescence detection.

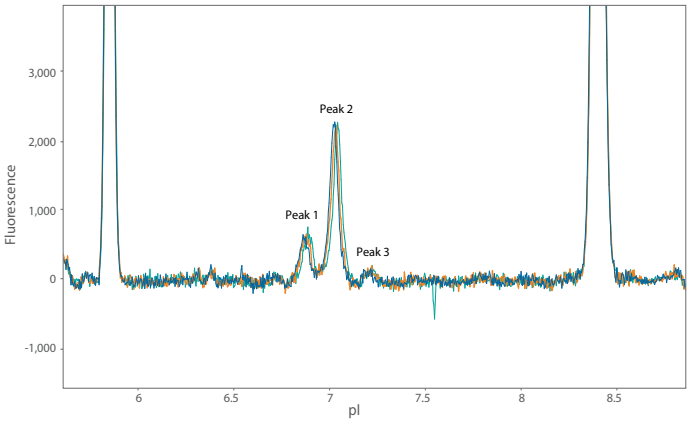

FIGURE 5. An overlay of three injections of denatured AAV6, run over the course of three days, visually demonstrates the inter-assay reproducibility of the denatured icIEF method.

PEAK %			
	PEAK 1	PEAK 2	PEAK 3
Day 1	22.7 22.7 22.6	75.3 74.7 73.0	2.0 2.6 4.4
Day 2	23.5 23.0 24.2	74.9 74.9 73.5	1.6 2.1 2.3
Day 3	19.7 19.4 20.2	77.3 78.5 78.0	3.0 2.0 1.8
Mean	22.0	75.6	2.4
%RSD	7.5	2.4	33.2

PEAK PI			
	PEAK 1	PEAK 2	PEAK 3
Day 1	6.86 6.87 6.89	7.03 7.03 7.04	7.21 7.22 7.22
Day 2	6.86 6.87 6.91	7.03 7.04 7.04	7.19 7.22 7.21
Day 3	6.91 6.89 6.89	7.05 7.05 7.06	7.23 7.24 7.27
STD	0.02	0.01	0.02

TABLE 4. Quantitative results from the nine injections of denatured AAV6, where triplicate injections were run on three different days, demonstrates the inter-assay reproducibility of the denatured AAV icIEF method. The results were very reproducible, as pI value standard deviation was all under 0.02 and %RSDs for percent peak area for peaks with greater than 10% composition were all under 7.5%.

USE MAURICE TO MONITOR AAV PARTICLE STABILITY

Temperature was used to stress-test intact or denatured AAV2 and AAV6 samples to determine whether Maurice could be used to monitor viral vector stability or capsid protein deamidation. We first evaluated the stress-tested intact AAV protein. A sample of AAV6 was treated at either 37 °C over the weekend, 50 °C for 10 minutes, or 60 °C for 10 minutes, and then compared to the reference AAV6 sample on Maurice using the intact method (**FIGURE 7**). The AAV6 particles were quite stable, remaining intact over the weekend at 37 °C or at 50 °C for 10 minutes. However, the AAV6 particle was not stable when it was stressed at 60 °C for 10 minutes, as we did not observe a peak signature at the same pI of the reference sample. AAV particles have been previously shown to have serotype-specific melting temperatures that range from 60–90 °C[2]. These data suggest the intact method for icIEF can be used to potentially monitor particle stability.

We then stressed denatured samples to determine whether Maurice could be used to monitor the stability of denatured viral samples. Denatured AAV2 and AAV6 samples were split into two aliquots – one aliquot was stressed at 95 °C for 5 minutes while the other aliquot was kept fresh on ice to be used as a reference sample. The stressed and reference samples were then analyzed on Maurice. A profile change was clearly observed with both AAV2 and AAV6 samples that were stressed with temperature, as there was an increase in acidic species, indicating icIEF analysis with Maurice can be used to monitor whether the sample has started to change (**FIGURE 8**). Quantitation of the peak area percent also indicates that the stressed sample has changed from the reference sample (**TABLE 5**) and, therefore, may have negative efficacy and safety implications if it's used as a delivery mechanism for gene therapy.

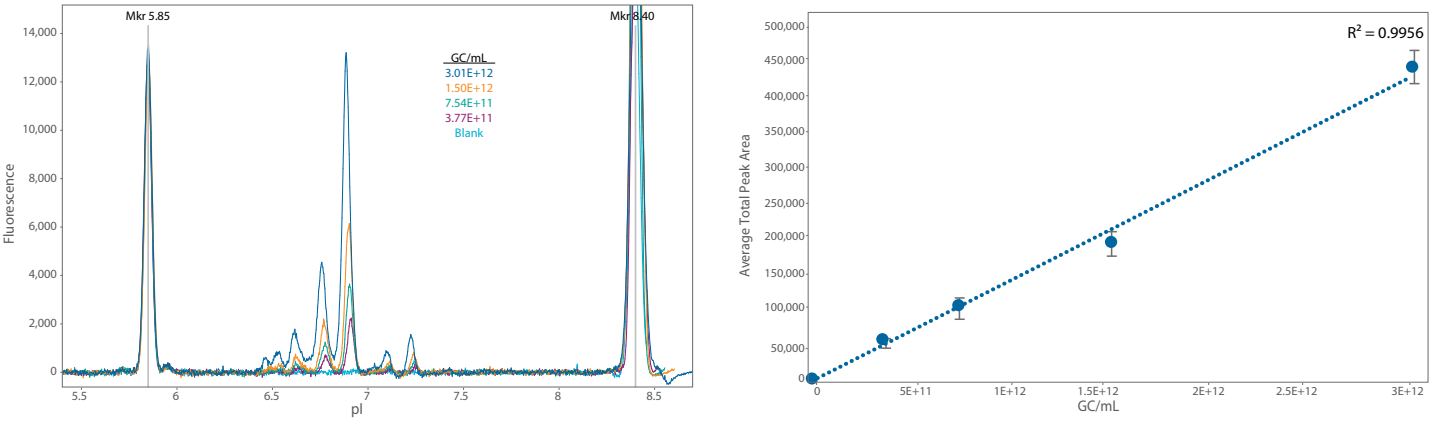

FIGURE 6. The denatured iciEF method for AAV2 is sensitive and shows good linearity. AAV2 was titrated from ~3 x 10^{12} down to 3 x 10^{11} GC/mL (top) and was detected with as little as 3 x 10^{11} GC/mL AAV2 using native fluorescence detection. Strong linearity was also observed (bottom) across the titration range tested with an R^2 of 0.9956.

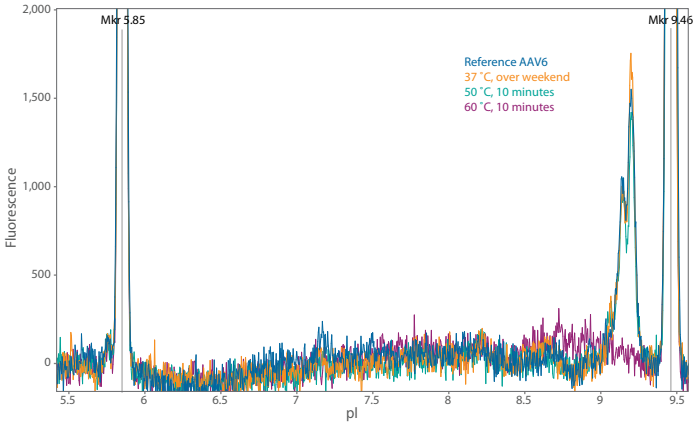

FIGURE 7. Intact AAV6 analysis following incubation at various temperatures. After 10 minutes at 60 °C, the AAV6 particle cannot be observed and is no longer stable. The change in peak signature after stress-testing indicates Maurice can be used to monitor viral vector stability.

MAURICE MONITORS AAV LOT-TO-LOT VARIATION

Finally, we evaluated whether Maurice icIEF native fluorescence could be used to monitor the lot-to-lot variation for identity in the viral vector source material. We obtained five different lots of AAV6, each with a different genomic content per mL (GC/mL) content and analyzed them with the intact icIEF methods on Maurice using native fluorescence (**FIGURE 9**). All five lots generated similar peak profiles at around pI ~9.25; however, an additional peak at a lower pI was observed in one lot, indicating the sample is different from the other four lots.

The total peak area for each lot was then graphed with the reported GC/mL to determine whether the Maurice AAV intact method shows a correlation between genomic content and protein composition (**FIGURE 10**). When the data were compared to the reported GC/mL from the vendor, the lots with the lower total peak area generally were the lots with lower GC/mL content.

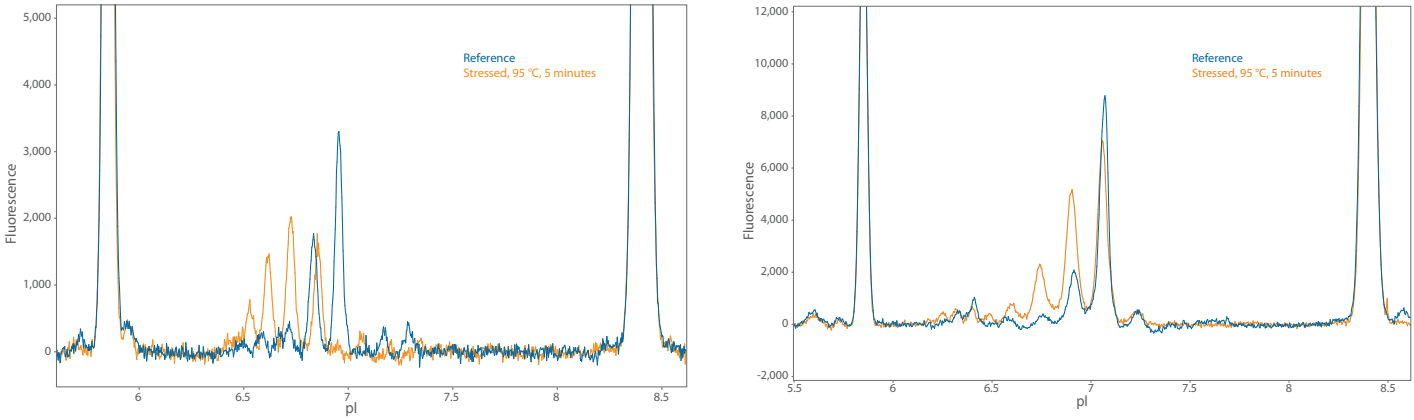

FIGURE 8. The stress-tested denatured AAV2 (left) and AAV6 (right) samples generated peak profiles that were significantly different compared to the reference sample using Maurice icIEF native fluorescence detection, indicating the stress-tested sample has changed. This indicates Maurice can be used to monitor the stability of denatured viral vector samples.

	AAV2 % PEAK AREA	
PEAK PI	REFERENCE SAMPLE	STRESSED SAMPLE
6.53	ND	11.8
6.59	4.1	24.3
6.72	7.1	35.4
6.83	28.5	25.2
6.95	50.5	2.7
7.17	3.8	0.6
7.29	6.0	ND

	AAV6 % PEAK AREA	
PEAK PI	REFERENCE SAMPLE	STRESSED SAMPLE
6.60	ND	4.7
6.74	ND	15.7
6.90	21.8	35.4
7.06	72.9	41.2
7.23	5.3	3.0

TABLE 5. Quantitation of % peak areas for the profiles generated when stressed and reference AAV2 (left) and AAV6 (right) samples were run on Maurice icIEF using native fluorescence detection support the conclusion that the stressing the sample at 95 °C for 5 minutes has changed the sample.

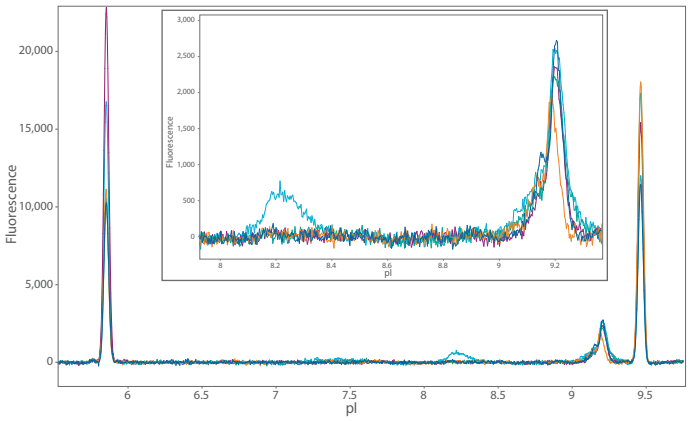

FIGURE 9. AAV6 lot-to-lot comparison. Five different lots of AAV6 were analyzed using the intact method. All lots produced a similar profile at pI ~ 9.25, but only one lot had an additional peak at a lower pI.

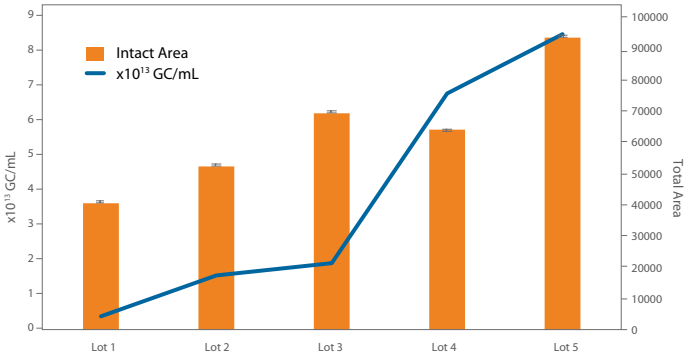

FIGURE 10. Comparison of AAV6 genomic copy and intact protein area. Each lot of AAV6 possessed a different genomic copy (GC/mL) number that ranged from 3.8 x 10^{12} – 8.53 x 10^{13} GC/mL, which was plotted against the intact AAV6 total peak area.

CONCLUSION

Charge heterogeneity is a critical quality attribute required by the FDA for every protein therapeutic to ensure drug safety and efficacy. The Maurice icIEF method delivers this analysis with a fully automated workflow that provides unprecedented reproducibility and sensitivity. This makes it an ideal system to characterize AAV vector stability for gene therapies. In this study, we demonstrated how Maurice can resolve either intact or denatured AAV2 and AAV6 isoforms using absorbance or native fluorescence detection. The data generated with native fluorescence, however, affords data with higher signal-to-noise ratios due to its improved sensitivity compared to absorbance detection, suggesting it should be the preferred detection mode when analyzing viral vector samples on Maurice.

Intra- and inter-assay quantitation using the total peak area was reproducible for both intact and denatured methods using fluorescence detection. The intra- and inter-assay total peak area RSDs were under 4.4% and 6.7%, respectively, for the intact method while intra- and inter-assay RSDs using either total peak area or % peak area were all under 7.6%. The quantitation was also highly linear with an R^2 of 0.9956 when denatured AAV2 was titrated from ~3 x 10^{12} GC/mL down to ~3 x 10^{11} GC/mL. We also subjected AAV2 and AAV6 samples to high temperature for accelerated stress tests to evaluate whether Maurice could be used to monitor vector stability. A change in peak profile was clearly observed in the stressed AAV2 and AAV6 sample when compared to the reference sample, using either the intact or denatured AAV method, indicating that charge heterogeneity analysis using Maurice can be used to monitor AAV stability. Finally, a comparison of five different lots of AAV material with different genomic content demonstrates that the Maurice intact AAV method can be used to monitor lot-to-lot variation between vector source material and inform on a lot's identity and protein content.

Maurice is a powerful platform that can be used to characterize your AAV viral vector to assess AAV lot-to-lot variability, concentration, and stability using stressed samples during the formulation phase of drug development. This means you'll always have the assurance that you're packaging your therapeutic RNA and DNA in a viral vector that will safely and efficiently deliver your drug treatment to the patient.

REFERENCES

1. Deamidation of amino acids on the surface of adeno-associated virus capsids leads to charge heterogeneity and altered vector function, A.R. Giles, J.J. Sims, K.B. Turner, L. Govindasamy, M.R. Alvira, M. Lock, J.M. Wilson, *Mol Ther*, 2018; **26**:2848-2862.

2. Thermal stability as a determinant of AAV serotype identity, A. Bennett, S. Patel, M. Mietzsch, A. Jose, B. Lins-Austin, J.C. Yu, B. Bothner, R. McKenna, M. Agbandje-McKenna, *Mol Ther Methods Clin Dev*, 2017; **6**:171-182.

Learn more | proteinsimple.com/maurice.html
Request price | proteinsimple.com/quote-request-ice-systems.html

CHAPTER 2: CHARACTERIZATION OF ADENO-ASSOCIATED VIRAL (AAV) VECTOR PROTEINS USING MAURICE CE-SDS

INTRODUCTION

The concept of gene therapy is straightforward in principle—find the gene(s) responsible for a specific disease state, introduce the proper copy, "fix" or normalize expression and rectify the ailment. In other words, use genes as medicine. Recent advances in vector engineering, delivery and safety have placed viral vector-based therapy at the forefront of gene therapy, with adeno-associated virus (AAV) being one of the most actively investigated. To that end, the first such gene therapy approved by the United States Food and Drug Administration (FDA), voretigene neparvovec-rzyl (Luxturna™), is an AAV serotype 2-based gene therapy for the treatment of mutation-associated blindness[1]. Another AAV-based drug treating X-linked retinal dystrophy is set to hit the market in the near future[2]. Beyond eye diseases, AAV-based gene delivery strategies are being applied in more than 200 clinical trials around the globe for diseases and disorders like hemophilia A and B, human immunodeficiency virus (HIV) infection, Parkinson's and Batten Disease, among others[3].

To support the rise of AAV vectors in the clinic, technological solutions that afford robust quality control assays are essential for implementing Good Manufacturing Practice (GMP), meeting regulatory requirements and ensuring the clinical quality, safety and consistency. In this chapter, we demonstrate how capillary electrophoresis sodium dodecyl sulfate (CE-SDS) can ensure these requirements are met. The state-of-art Maurice™ system delivers CE-SDS analysis with excellent specificity, linearity, repeatability and quantification of your AAV samples, and with the ability to detect impurities.

WHY USE MAURICE OVER OTHER CE-SDS PLATFORMS FOR AAV PURITY ANALYSIS?

CE-SDS is a standard method for protein separations and analyses in most biological research laboratories. It is widely used for release and stability analysis of biotherapeutic proteins, to demonstrate product purity, identity, consistency and shelf life during the manufacturing and life cycle of the product. The Maurice and Maurice S. systems from ProteinSimple transform conventional CE-SDS separation and analysis with a fully automated, vastly simpler workflow that results in highly robust, high-quality data.

In this study we demonstrate the benefit of the Maurice system for rapid and well-resolved product characterization of AAV capsid protein, by confirming the purity of the product, and the ratio of the three AAV viral proteins, VP1, VP2 and VP3, within a product.

MATERIALS & METHODS

AAV2 (8 x 10^{13} GC/mL) samples were obtained from Vigene Biosciences. The CE-SDS 25X Internal Standard (IS), Maurice CE-SDS PLUS 1X Sample Buffer and the running reagents were all obtained from the ProteinSimple Maurice CE-SDS PLUS Application Kit (PN PS-MAK03-S). Tris(2-carboxyethyl)phosphine (TCEP) from Thermo Scientific (PN A35349) was reconstituted using HPLC grade deionized water to a stock concentration of 40 mM. Sodium dodecyl sulfate 20% (SDS) was purchased from BioRad (PN 1610418). Sartorius Vivaspin 500 Centrifugal Concentrators 30 kDa were purchased from Thermo Scientific (PN 14-558-400). Illustra NAP-5 Columns were purchased from GE Healthcare (PN 17085302). Foil plate seals were purchased from E&K Scientific Products (PN T790100). Additionally, 10X PBS (PN P5493), Poloxamer 188 10% solution (PN P5556) and β-mercaptoethanol (β-ME) (PN M3148) were purchased from MilliporeSigma.

DENATURED AAV ANALYSIS

As opposed to intact analysis, denatured AAV analysis enables the quantification of individual viral capsid proteins, VP1, VP2, and VP3, to quantify their ratios. The standard AAV samples were desalted with Vivaspin 500 spin columns by diluting 100 µL of AAV sample into 500 µL of 0.001% poloxamer 188 and concentrated to 50 µL. The linearity samples were buffer exchanged with NAP5 columns into 15 mM PBS in 0.001% poloxamer 188. The NAP5 columns were loaded with 100 µL of sample, chased with 400 µL of buffer and the final 500 µL was collected before concentrated to 50 µL. The linearity samples were diluted into the same buffer to maintain a constant salt concentration across the linearity sample range. The resulting concentrations were 1.6 x 10^{14} GC/mL, 1.3 x 10^{14} GC/mL, 1.1 x 10^{14} GC/mL, 8.0 x 10^{13} GC/mL and 5.3 x 10^{13} GC/mL in a total volume of 10 µL per sample. For all samples, 20% BioRad SDS solution was added to Maurice CE-SDS PLUS Sample Buffer to a final concentration of 4% SDS. TCEP was also added to this mixture to make a 4 mM final solution as well as the CE-SDS 25X Internal Standard for a 0.5X final solution. Then, we added 2.5 µL of this premixed sample buffer to 7.5 µL of sample in a 96-well plate. The samples were covered with a foil plate seals and denatured at 70 °C for 10 minutes, cooled to RT for 5 minutes, and mixed by vortex.

Samples were prepared for Maurice analysis by diluting the denatured samples with 30 µL of water. The 96-well plate was spun down in a centrifuge for 10 minutes at 1000 x *g*. Samples were injected for 15 seconds at 4600 V and separated using a Maurice CE-SDS PLUS Cartridge (PN PS-MC02-SP) for 30 minutes at 5750 V. Absorbance at 220 nm was captured and analyzed using Compass for iCE software. For the AAV capsid ratio assessment method, neat (untreated) AAV2 samples were used instead of concentrated samples, a final concentration of 2.5% β-ME was used instead of TCEP, the internal standard was omitted, and the injection was modified to 20 seconds at 5000 V.

RESULTS

SPECIFICITY

To show the specificity of the CE-SDS method for AAV purity analysis, the AAV2 sample was analyzed on Maurice and compared to a blank sample preparation. The resulting electropherograms (e-grams) were overlaid, revealing the clear presence of AAV2 and no interfering peaks in the blank sample (**FIGURE 11**). Importantly, the three capsid proteins (VP1, VP2 and VP3) were clearly separated from one another, with a baseline signal between each of them. This allows for accurate quantification of each protein peak area (see the Repeatability test below). Several minor low molecular weight species were observed, indicating the presence of impurities. These data suggest that the CE-SDS method is specific for AAV analysis, allowing for clear separation of individual capsid proteins, as well as detection of the presence of impurities.

LINEARITY

We assessed the linearity of the CE-SDS assay for AAV2 analysis across a dilution series from 1.6 x 10^{14} GC/mL to 5.3 x 10^{13} GC/mL. A sample from each concentration was injected three times and the total peak area for the three capsid proteins results were averaged for each concentration. Representative e-grams from this analysis showed a change in peak area for the three capsid proteins that correlated with the sample concentration (**FIGURE 12**). This analysis showed that total peak area had a strong linear correlation across the dilution series with an R^2 value of 0.9852 (**Figure 13**). When omitting the highest (1.6 x 10^{14} GC/mL) concentration, the linearity correlation was even stronger, with an R^2 value of 0.9914 (**FIGURE 13**). Across the linearity test, the average capsid ratio was 8.1:1.3:1 for VP3, VP2 and VP1, respectively. These data suggest that the CE-SDS assay for AAV analysis is applicable across a wide dynamic range.

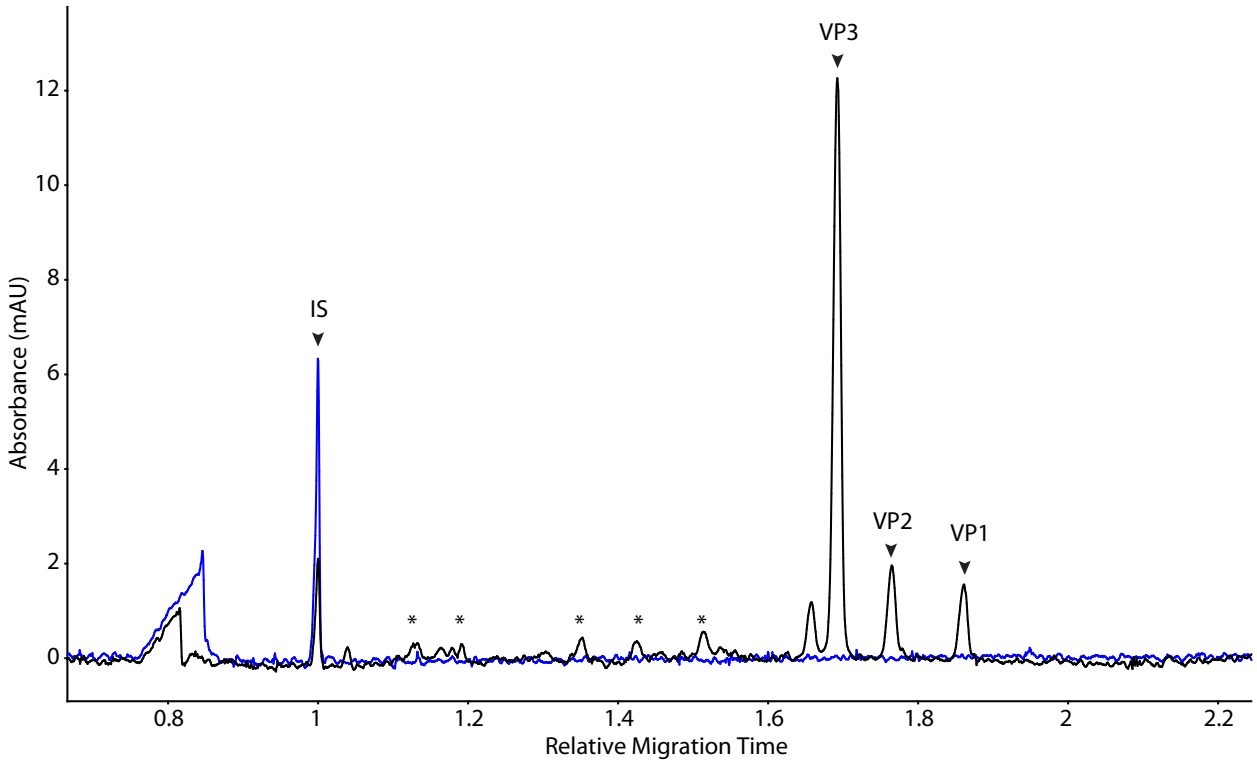

FIGURE 11. Maurice CE-SDS method detects and resolves AAV capsid proteins. The AAV2 sample is shown in the black trace and the blank sample is shown in the blue trace. The internal standard is labeled as IS and impurities are labeled with an asterisk.

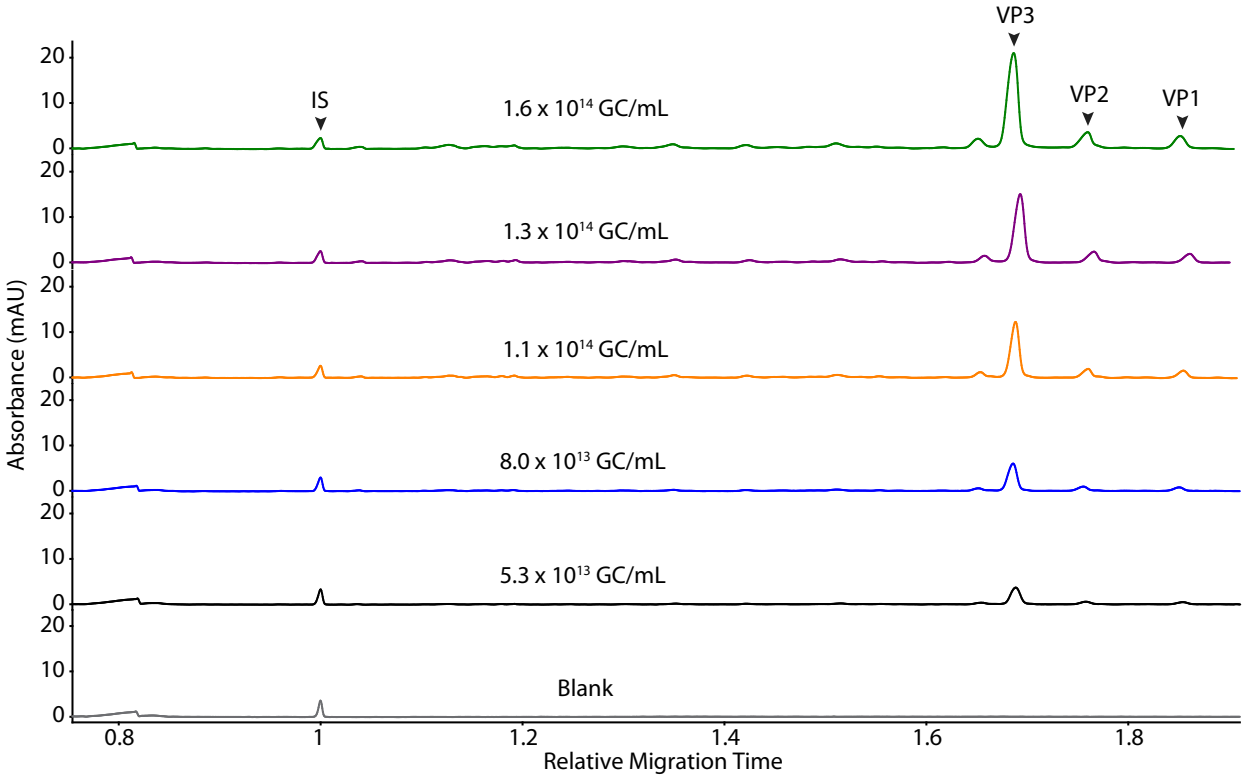

FIGURE 12. Representative CE-SDS electropherograms from AAV titration. AAV2 was diluted from 1.6 x 10^{14} GC/mL (green trace) to 5.3 x 10^{13} GC/mL (black trace). The bottom (gray) trace is the sample blank. The internal standard is labeled as IS.

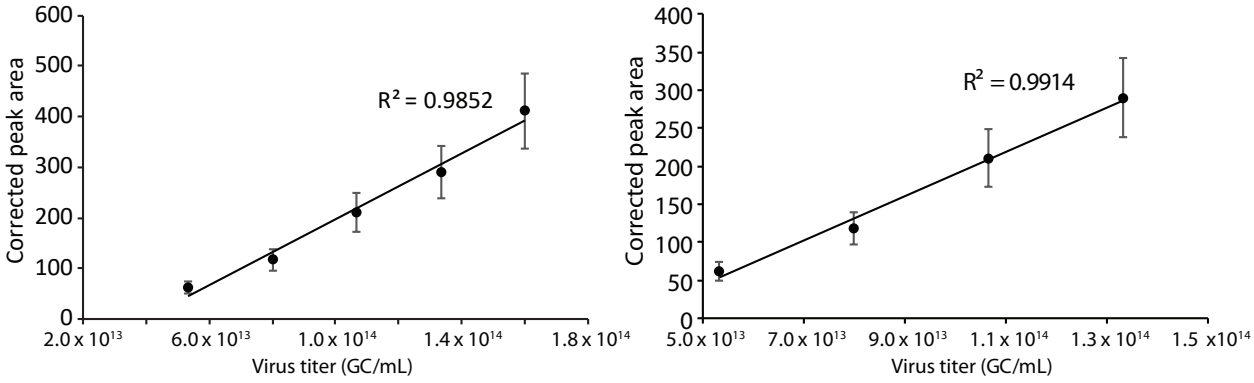

FIGURE 13. The CE-SDS method for AAV analysis shows good linearity. AAV2 was diluted from 1.6 x 10^{14} GC/mL to 5.3 x 10^{13} GC/mL and analyzed on Maurice. The left graph includes all concentrations and the right graph has the highest concentration (1.6 x 10^{14} GC/mL) omitted. The data points represent the total peak area averages of three replicate injections, and error bars represent the standard errors of the averages.

REPEATABILITY

To test the repeatability of the CE-SDS method, we performed five replicate injections of the AAV2 sample. As expected, the electropherograms that resulted from this analysis were qualitatively identical to one another (**FIGURE 14**). The peak area percentages of VP3, VP2 and VP1 and their respective ratios were calculated (**TABLE 6**). The results showed excellent repeatability with percent relative standard deviations (%RSDs) of 0.5%, 4.0%, and 4.3% for VP3, VP2 and VP1, respectively. The average capsid ratios were 7.6:1.3:1 for VP3:VP2:VP1. These data suggest that the CE-SDS method for AAV analysis is quantitative and has high repeatability.

	% CORRECTED PEAK AREA			CAPSID PEAK AREA		
INJECTION NAME	VP3	VP2	VP1	VP3	VP2	VP1
Injection 1	71.6	12.4	8.9	8.0	1.4	1.0
Injection 2	71.0	12.8	9.7	7.3	1.3	1.0
Injection 3	71.3	12.5	9.0	7.9	1.4	1.0
Injection 4	70.8	11.7	9.9	7.2	1.2	1.0
Injection 5	70.6	13.2	9.1	7.8	1.5	1.0
Average	71.1	12.5	9.3	7.6	1.3	1.0
%RSD	0.5	4.0	4.3	4.5	6.9	0.0

TABLE 6. CE-SDS quantitation for AAV analysis is reproducible. The AAV2 sample was injected as five replicates and the percent peak area for each capsid protein and their respective ratios were calculated.

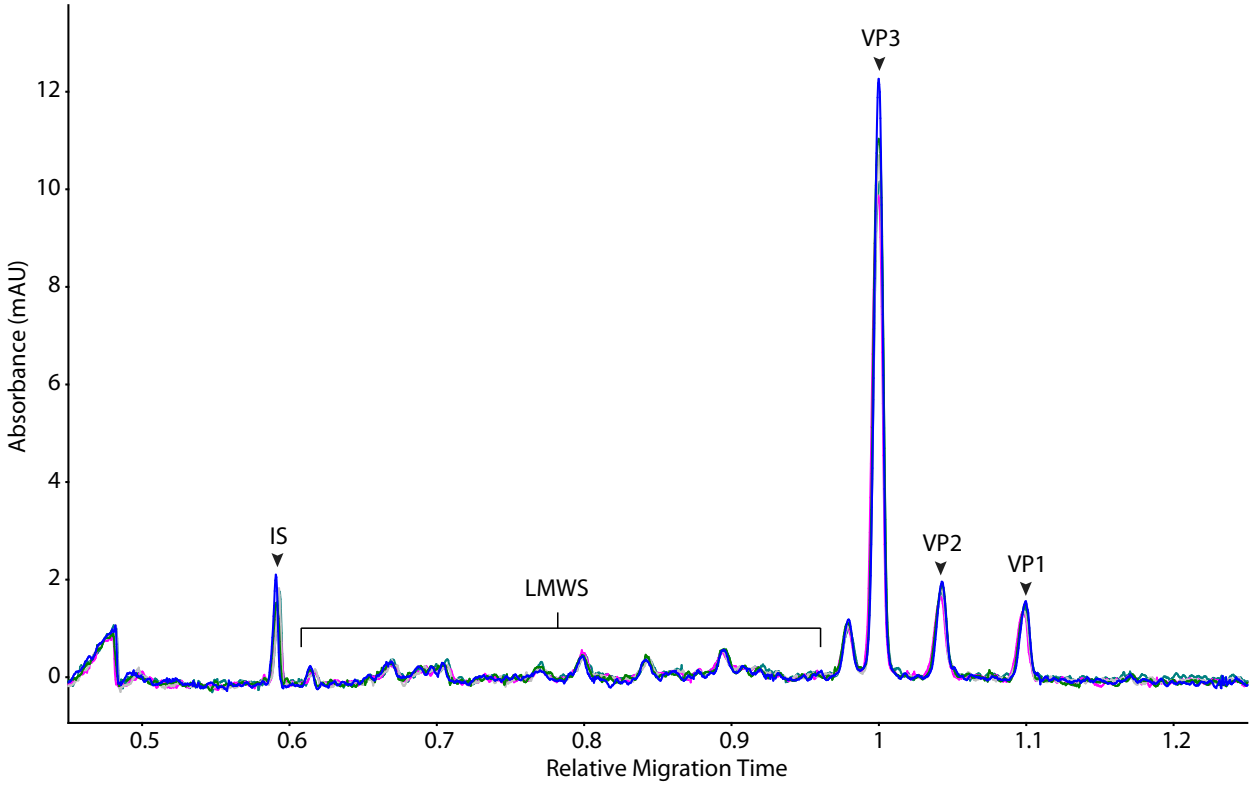

FIGURE 14. Five replicate injections using the CE-SDS method for AAV analysis. The AAV2 sample was injected in five replicates. The internal standard is labeled as IS. LMWS: low molecular weight species.

ANALYSIS OF UNTREATED AAV SAMPLES

The results presented so far were performed with treated AAV2 samples that contained low salt and high protein concentration. We next assessed how the CE-SDS method could perform on AAV2 samples in their original vendor formula of 1X PBS, which are comparatively lower in protein and higher in salt concentration. Two samples of untreated AAV2 were prepared, and each sample preparation was injected three times. A representative electropherogram from this analysis is shown in FIGURE 15. Because the protein concentration is lower in this method, the minor low molecular weight species were not observed, but the main AAV peaks were still present, clearly separated and quantifiable. Additionally, two shoulder peaks were resolved from the main VP3 peak. The peak area of the VP3, VP2 and VP1 from each injection were recorded, and the averages and %RSDs were calculated (TABLE 7). The results showed a %RSD of 0.76, 4.03, and 4.86 percent and capsid ratio of 7.9:1.3:1 for VP3, VP2 and VP1, respectively. These data suggest that the CE-SDS method can quickly and easily characterize AAV2 particles without the need for extensive pretreatment.

	% CORRECTED PEAK AREA			CAPSID PEAK AREA		
INJECTION NAME	VP3	VP2	VP1	VP3	VP2	VP1
Sample 1, Rep1	78.9	11.6	9.5	8.3	1.2	1.0
Sample 1, Rep2	77.6	12.1	10.3	7.5	1.2	1.0
Sample 1, Rep3	77.8	13.0	9.2	8.5	1.4	1.0
Sample 2, Rep1	76.9	12.8	10.3	7.5	1.2	1.0
Sample 2, Rep2	77.9	12.8	9.3	8.4	1.4	1.0
Sample 2, Rep3	77.7	12.1	10.2	7.6	1.2	1.0
Average	77.8	12.4	9.8	7.9	1.3	1.0
%RSD	0.8	4.0	4.9	5.3	7.3	0.0

TABLE 7. Quantitative results for replicate injections from CE-SDS analysis of untreated AAV2 samples. Two sample preparations were injected three times each.

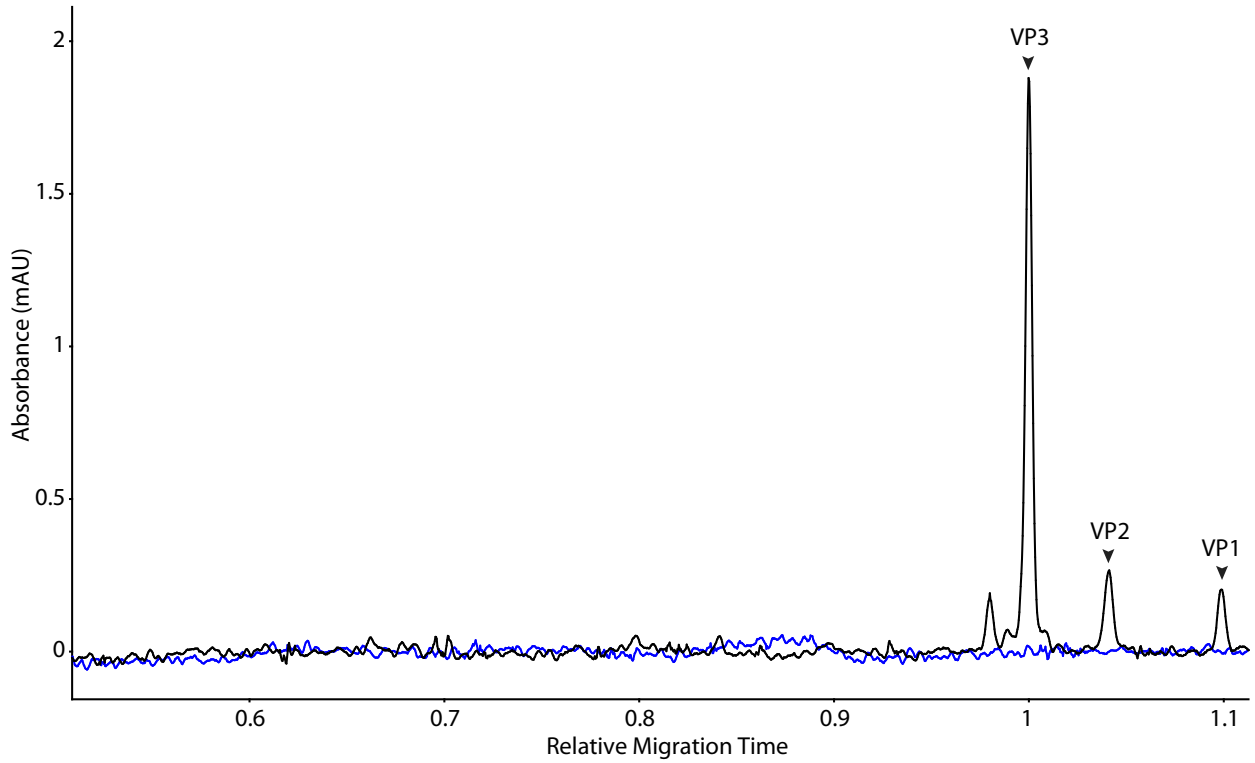

FIGURE 15. CE-SDS analysis of untreated AAV2 samples. The AAV2 sample is shown in the black trace and the blank sample is shown in the blue trace. All three viral capsid proteins are detected.

CONCLUSION

We developed a CE-SDS assay for AAV capsid purity assessment on the Maurice system to support gene therapy process development and characterization. Unlike traditional SDS-PAGE, which is labor-intensive, poorly reproducible and semi-quantitative at best, the CE-SDS method is more sensitive, quantitative and consistent. Maurice takes conventional CE-SDS to another level by delivering unparalleled ease of use, automation and superior assay performance. Simply load the cartridge and samples, then start the batch. The method demonstrated complete separation of the three AAV capsid proteins and provided quantitative results that had a wide dynamic range with excellent repeatability. Importantly, the method could reveal minor low molecular weight impurities in the AAV samples. Maurice can also analyze untreated AAV samples with low protein and high salt concentration, without compromising repeatability.

In summary, we demonstrate here that Maurice provides a powerful solution for CE-SDS analysis of AAV capsid proteins. Additionally, Maurice icIEF method delivers charge heterogeneity analysis of AAV with unprecedented reproducibility and sensitivity (see Chapter 1 on icIEF analysis of Adeno-Associated Virus (AAV) proteins for Gene Therapy), making Maurice an ideal platform for characterization of viral vector proteins.

REFERENCES

1. Voretigene Neparvovec: An emerging gene therapy for the treatment of inherited blindness, U. Patel, M. Boucher, L. Léséleuc and S. Visintini, *CADTH Issues in Emerging Health Technologies* 2018; 169.

2. Pharmaceutical Development of AAV-Based Gene Therapy Products for the Eye, G.A. Rodrigues, E. Shalaev, T.K. Karami, J. Cunningham, N.K.H. Slater and H.M. Rivers, *Pharmaceutical Research*, 2019; **36**:29.

3. Gene therapy leaves a vicious cycle, R. Goswami, G. Subramanian, L. Silayeva, I. Newkirk, D. Doctor, K. Chawla, S. Chattopadhyay, D. Chandra, N. Chilukuri and V. Betapudi, *Frontiers in Oncology*, 2019; **9**:297.

On-Demand Webinar - Innovative Capillary Electrophoresis Techniques for Gene Therapy R&D

Learn more | proteinsimple.com/maurice.html
Request price | proteinsimple.com/quote-request-ice-systems.html

CHAPTER 3: SIMPLE WESTERN ANALYSIS OF ADENO-ASSOCIATED VIRUS (AAV) PROTEINS FOR CELL AND GENE THERAPY

Nishant Pawa, Ph.D., Anusha Seneviratne, Ph.D. and Tony Bou Kheir, Ph.D., Cell and Gene Therapy Catapult, London, United Kingdom

Caroline Odenwald, Ph.D. and Katja Betts, EMSc, PROGEN, Heidelberg, Baden-Württemberg, Germany

Chris Heger, Ph.D., Yasef Khan, Charles Haitjema, Ph.D. and Daniela Ventro, Ph.D., ProteinSimple, San Jose, CA, USA

INTRODUCTION

In gene therapy, a therapeutic transgene is delivered to cells and patient tissues to treat an inherited or developed disease. This genetic reprogramming is typically achieved with viral vectors, the most promising of which is the adeno-associated viruses (AAV)[1]. As a safe and effective vector, AAV is the workhorse of *in vivo* gene therapy, with three approved products and many more currently in clinical trials[1,2]. An AAV particle is composed of 60 capsid protein molecules, with subunits of VP1, VP2 and VP3 at a ratio of 1:1:10[1]. The subunits are encoded by the *cap* gene and are created by alternative splicing and translation from different start codons.

During AAV manufacturing, critical quality attributes must be monitored, including the presence, identity and purity of viral vector proteins[3]. Traditionally, the identity of these proteins is monitored by Western blot using sodium dodecyl sulfate polyacrylamide gel electrophoresis (SDS-PAGE). However, Western blotting is notoriously challenging; it's labor-intensive, suffers from poor reproducibility, and is only semi-quantitative. For this reason, the Cell and Gene Therapy Catapult (CGTC), an independent center of excellence at the forefront of technology and innovation for C&GT commercialization, is adopting next generation technologies to advance quality control (QC) of AAV-mediated gene therapy[3]. In this chapter, you'll see how CGTC has used highly-specific antibodies exclusively manufactured by PROGEN with fully automated Simple Western™ assays on Wes™ to monitor and characterize AAV capsids during product purification.

HOW SIMPLE WESTERN DOES AAV PROTEIN ANALYSIS BETTER

Simple Western assays are fully automated, capillary-based immunoassays that separate and analyze proteins by size from 2 kDa to 440 kDa. Unlike traditional Western blotting methods, this means Simple Western assays are reproducible and quantitative. They require only 3 µL of your sample to get picogram-level sensitivity and automatically analyzed results within 3 hours! These are major advantages for the analysis of AAVs, which are difficult to manufacture and for which demand currently outpaces supply[4]. And, with 21 CFR 11-compliant Compass for Simple Western software, you'll be all set for adoption of Simple Western in a good manufacturing practice (GMP) environment. In a nutshell, Simple Western assays are easy-to-use, low-waste and single-use immunoassays that reduce the time and complexity of AAV manufacturing workflows!

Simple Western plugs and plays throughout the AAV product development pipeline, from measuring the expression of novel AAV capsids, to downstream manufacturing and QC, where accurately measuring product identity and purity are imperative[3]. Herein, AAV capsid proteins were clearly separated and identified via Simple Western assays on Wes. Total protein was also monitored to detect the presence of process-related protein impurities during purification, making Wes a valuable tool for the advancement of QC workflows for AAV-based gene therapies.

MATERIALS & METHODS

The default Wes sample preparation and assay conditions were followed using the 12–230 kDa Wes Separation Module (PN SM-W004) and the Anti-Mouse Detection Module (PN DM-002). For total protein detection, the instructions were followed in the Total Protein Detection Module for Wes (PN DM-TP01). Anti-AAV VP1/VP2/VP3 mouse monoclonal (PN 61058), anti-AAV2 VP1/VP2 mouse monoclonal (PN 61057) and anti-AAV2 VP1 mouse monoclonal (PN 61056) antibodies were obtained from PROGEN. AAV2 was purchased from Vigene Biosciences (custom order), or internally produced and purified at CGTC.

IDENTIFICATION OF VP1/2/3 DURING AAV PURIFICATION

AAV2 was purified from whole HEK293 cell lysate using affinity chromatography, and the steps of the purification process (load, flow-through, wash and elution) were monitored on Wes. This analysis showed the presence of VP1, VP2 and VP3 proteins in the elution fraction using the immunoassay (**FIGURE 16A**) and total protein (**FIGURE 16B**). Less dilute samples were loaded for the immunoassay to detect low abundance immuno-reactive species. Closer analysis of the elution fraction revealed that the signal intensity of VP1 and VP2 were approximately equal, while VP3 had a significantly stronger signal (**FIGURE 17**).

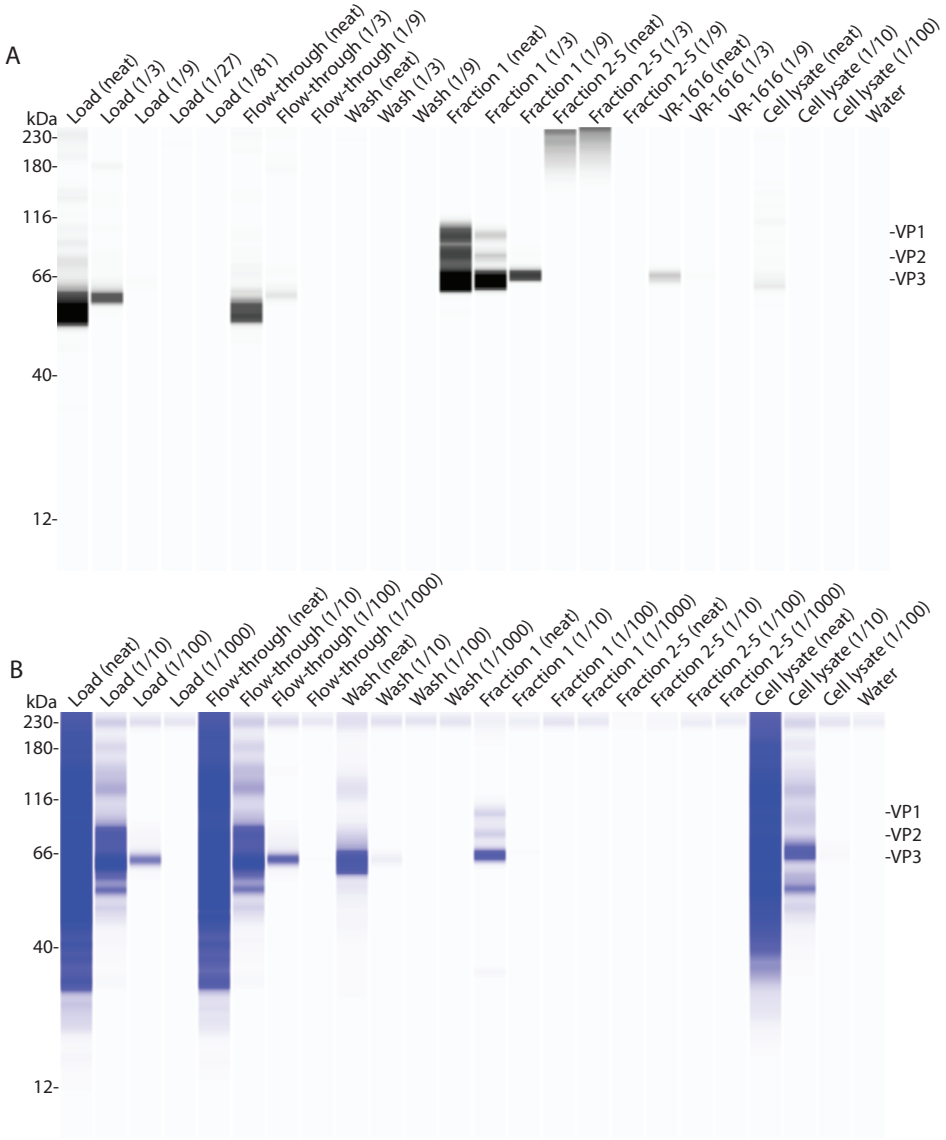

FIGURE 16 (A) Immunodetection of VP1, VP2 and VP3 proteins during purification from whole-cell lysate. Detection was performed with an anti-AAV VP1/VP2/VP3 mouse monoclonal antibody. (B) Total protein detection of each fraction. Load: input material loaded onto the columns; flow-through: material not bound on columns; wash: wash buffer from columns; fractions: eluate fractions from columns; VR1616: ATCC purified reference material loaded as a positive control (low titer); cell lysate: HEK293 cell lysate (without virus); water: negative control. Sample dilutions are shown in brackets.

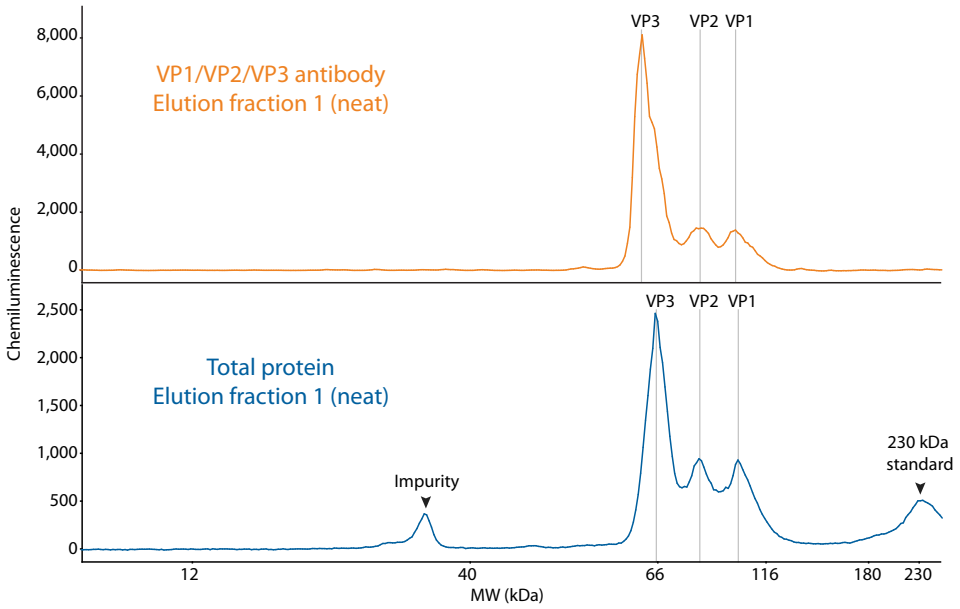

FIGURE 17. Electropherogram analysis of the elution fraction from the immunoassay (top panel) and total protein analysis (bottom panel). The immunoassay detection was performed with an anti-AAV VP1/VP2/VP3 mouse monoclonal antibody.

The total protein analysis of this fraction also showed an impurity of just under 40 kDa and the presence of the 230 kDa internal standard, whose presence is expected (**FIGURE 17**). The detection of impurities shows that Simple Western assays can also be used for bioprocess contaminant detection, including host cell proteins, and purification or media additives. Appropriate for these purposes, Simple Western assay sensitivity on Wes rivals traditional approaches, such as ELISA, and also provides information on molecular weight, degraded products, and oligomerization state, among other attributes.

The results presented in **FIGURE 16** and **FIGURE 17** leverage a single antibody anti-AAV VP1/VP2/VP3 mouse monoclonal antibody that detects all three AAV capsid subunits. Wes is an open platform amenable to any antibody, meaning other targets may be detected simply by swapping in different antibodies. For example, to detect specific capsid proteins, antibodies targeting AAV capsid proteins VP1/VP2/VP3, VP1/VP2 or VP1 were screened against commercially available AAV2 (**FIGURE 18**), enabling the identification of individual proteins in addition to all three. Because up to 25 different antibodies may be tested on a single Wes run, screening multiple antibodies is straightforward with Simple Western assays.

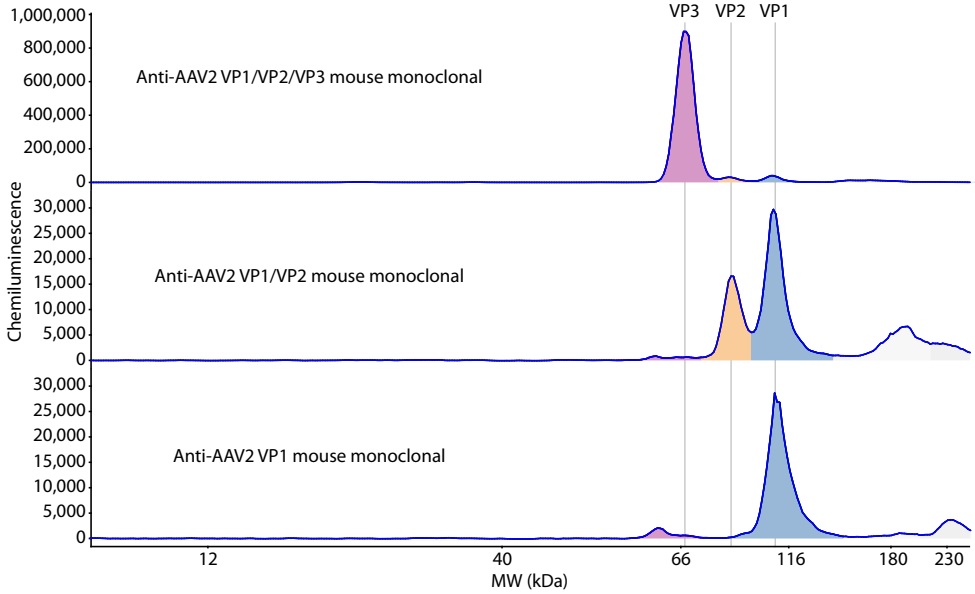

FIGURE 18. Antibody screen targeting VP1/VP2/VP3 proteins (top panel), VP1/VP2 proteins (middle panel) and VP1 only (bottom panel).

To determine the range of detection, commercially available AAV2 (1 x 10^{13} GC/mL, 33.8 µg/mL) was subjected to a 2X dilution series from 1:8 to 1:256 and analyzed on Wes. The anti-AAV VP1/VP2/VP3 mouse monoclonal antibody was used to detect each capsid protein (**FIGURE 19A**). The total peak area of VP1/VP2/VP3 was calculated and plotted at each dilution factor (**FIGURE 19B**). This analysis indicated that detection of AAV proteins was possible right down to the lowest dilution tested of 1:256 (**FIGURE 19B**). Thus, Simple Western assays allow for sensitive detection of target proteins, as this corresponds to just 400 pg of protein loaded per well.

CONCLUSION

Simple Western assays are automated immunoassays also capable of total protein analysis, which greatly simplifies AAV product development workflows. In less than 3 hours, you can analyze up to 25 samples per run on Wes—all in a fully automated fashion! These advantages, combined with the small sample size requirement (3 µL), make Simple Western a powerful analytical tool throughout the AAV product development pipeline. For example, Wes can be applied for small scale testing and formulation in small bioreactors, allowing for process monitoring and optimization without sacrificing large amounts of precious sample. Here, AAV capsid proteins were monitored and quantitated on Wes during purification from whole-cell lysate. The VP1, VP2 and VP3 capsid proteins could be detected and measured either individually or simultaneously, depending on the AAV antibody used for detection. In addition to identity, other critical quality attributes to consider in AAV manufacturing include purity, potency, stability and safety. With additional antibodies, Simple Western assays can be extended to address these other attributes, including for measuring host cell proteins (purity), target protein expression (potency), presence over time (stability) and contaminants like Mycoplasma (safety).

Webinar - The Next Generation of AAV Characterization Tools

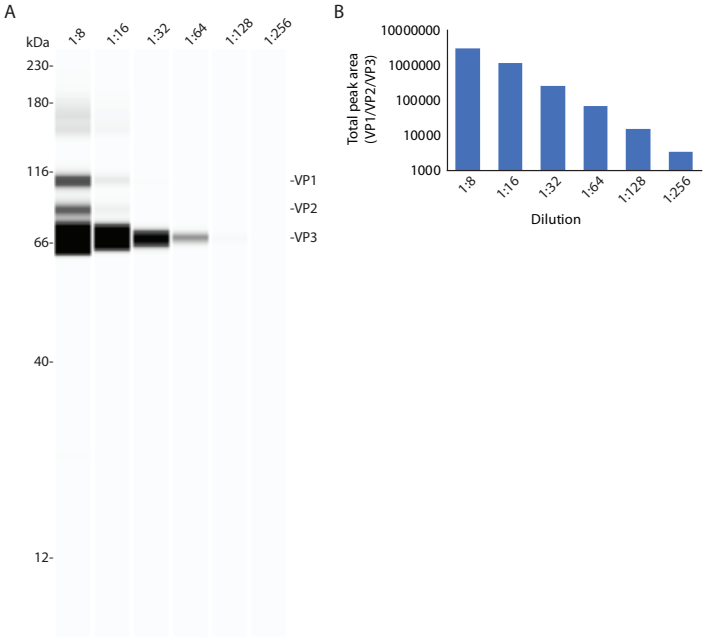

FIGURE 19. Range of detection of the anti-AAV VP1/VP2/VP3 mouse monoclonal antibody. (A) Lane view of VP1/VP2/VP3 detection of each dilution. (B) Total peak area of VP1/VP2/VP3 by dilution factor.

REFERENCES

1. Adeno-associated virus vector as a platform for gene therapy delivery, D. Wang, P. Tai and G. Gao, *Nature Reviews Drug Discovery*, 2019; **18**:358–378.

2. Onasemnogene Abeparvovec: First global approval, S. Hoy, *Drugs*, 2019; **79**:1255–1262.

3. AAV next generation quality control, T. Kheir, *Cell and Gene Therapy Catapult*, 2019.

4. Development of a scalable platform for AAV manufacturing, J. Guenat, A. Soula, F. Leseigneur, Q. Bazot, N. Weeratunge, N. Pawa, L. Li, T. Kheir, G. Berger, T. Thwaites, M. Delahaye, J. Kerby, H. Mirmalek-Sani and J. Appleby, *Cell and Gene Therapy Catapult*, 2019.

ACKNOWLEDGMENT

This work was funded by Innovate UK, and performed in collaboration with Professor Farzin Farzaneh's group at Kings College London and Guys & St Thomas NHS Foundation Trust (GSTT).

Learn more | proteinsimple.com/simple_western_overview.html
Request pricing | proteinsimple.com/quote-request-simple-western-systems.html

CHAPTER 4: CONCENTRATING ON AAV IMPURITIES WITH ULTRASENSITIVE TOTAL PROTEIN DETECTION ON SIMPLE WESTERN

TOTAL PROTEIN DETECTION WITH SIMPLE WESTERN

Impurities in protein products can be dangerous and impact efficacy. For example, protein impurities in final drug products could lead to undesirable immune responses in patients, so detecting total protein is critical for revealing impurities in preparative protein production. Traditional methods for total protein detection rely on SDS-PAGE with dyes like Coomassie Blue, SYPRO Ruby, or silver stain. However, SDS-PAGE requires large sample volumes, a lot of hands-on time, and it is poorly reproducible. Also, the use of staining dyes often comes with a lot of waste and can require specialized imaging equipment to which not every researcher has access.

Conversely, Simple Western™ assays on instruments like Jess and Wes from ProteinSimple offer fully automated protein separation and quantification with small sample volumes, and sensitive chemiluminescent-based immunodetection and total protein detection. While immunoassays on Simple Western allow target-specific detection, the Total Protein Detection Module (**FIGURE 20**) allows for all proteins to be labeled and detected, which is ideal for monitoring impurities. Here, we show that total protein detection with Simple Western can be even more sensitive by using 5 times more concentrated biotin labeling reagent, resulting in protein detection that surpasses the sensitivity of protein stains like SYPRO Ruby. While SYPRO Ruby requires at least 1 ng of protein for reliable detection,[1-2] Simple Western can reliably detect as little as 150 pg. This SYPRO Ruby-beating sensitivity improvement makes Simple Western well suited for the analysis of precious samples such as Adeno-Associated Virus (AAV) samples used in Cell & Gene Therapy workflows.

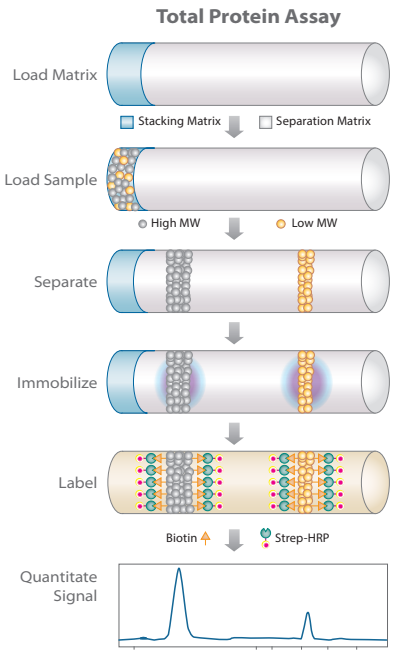

FIGURE 20. How the Total Protein Detection Assay works

SIMPLE WESTERN IS A MULTI-ATTRIBUTE METHOD

Identity and purity are among the critical quality attributes (CQAs) that must be monitored during AAV manufacturing. While ELISA can provide identity information, it cannot provide purity information in the same assay. In this regard, ELISA is a single-attribute method. By contrast, Simple Western is a multi-attribute method because it can deliver both identity and purity in the same assay. For example, identity can be achieved with antibodies specific to VP1/VP2/VP3 capsid proteins, while purity may be achieved with total protein detection, which now rivals the sensitivity of the best gel staining techniques. In this chapter, we show how to achieve ultrasensitive total protein detection using the 5X biotin labeling reagent with a focus on AAV analysis.

MATERIALS AND METHODS

The reagents used in this study are listed in TABLE 8.

PREPARING THE 1X AND 5X LABELING REAGENT

To prepare 1X biotin labeling reagent, the default instructions provided with the Total Protein Detection Module were followed. To prepare the 5X biotin labeling reagent, 30 µL of Reconstitution Agent 1 were added per tube (instead of 150 µL for a 1X concentration). Then, this solution was mixed 1:1 with Reconstitution Agent 2. For RePlex analysis, the default instructions provided with the RePlex module were followed.

PREPARING THE SAMPLES

To analyze rDnaK (Enzo Life Sciences), a 3-fold serial dilution series was prepared in 1X master mixture (MM) and denatured under reducing conditions for 5 minutes at 95 °C. The concentrations in the dilution series were 100, 33.3, 11.1, 3.7, 1.23, 0.41, 0.14, 0.046, 0.015 and 0 µg/mL.

AAV2 (Vigene Biosciences) spiked with RNase A was prepared in 1X MM and denatured under reducing conditions for 10 minutes at 70 °C. The AAV2 (Vigene Biosciences) was diluted at 1:10 and the RNase A at 10, 3.33, 1.11, 0.37, 0.123 and 0 µg/mL. AAVs analyzed on RePlex were prepared at 1:20 concentration in 1X MM (with 2-40 kDa FI Standards) and denatured under reducing conditions for 10 minutes at 70 °C.

NAME	VENDOR	PART NUMBER
12-230 kDa Jess or Wes Separation Module	ProteinSimple	SM-W004
Total Protein Detection Module	ProteinSimple	DM-TP01
RePlex™ Module	ProteinSimple	RP001
Bicine/Chaps Lysis Buffer and Sample Diluent	ProteinSimple	040-764
DnaK (E. coli), (recombinant)	Enzo Life Sciences	ADI-SPP-630
AAV2-CMV-GFP	Vigene Biosciences	CV10004
RNase A	Sigma Aldrich	R5250
anti-AAV VP1 mouse monoclonal, A1, lyophilized, purified	Progen	61056
anti-AAV VP1/VP2/VP3 mouse monoclonal, B1, lyophilized, purified	Progen/Origene	61058/BM5015
10% Criterion™ TGX™ Precast Midi Protein Gel, 26 well, 15 µl	Bio-Rad	5671035
Precision Plus Protein Dual Standards Ladder	Bio-Rad	1610377
4X Laemmli Buffer	Bio-Rad	1610747
10x Tris/Glycine/SDS Buffer	Bio-Rad	1610732
SYPRO® Ruby Protein Gel Stain	ThermoFisher	S12000

TABLE 8. Reagents used in this study. The anti-AAV VP1 and anti-AAV VP1/VP2/VP3 antibodies were diluted 1:20 and 1:50 in Antibody Diluent 2, respectively.

COMPARING 5X LABELING REAGENT TO SYPRO RUBY

AAV2 (1 x 10^{13} GC/mL) was prepared in 2X serial dilution series from 1:5 to 1:160. Each dilution was labeled with 5X labeling reagent and analyzed on Wes in duplicate using the 12-230 kDa Separation Module and the Total Protein Detection Module under default conditions. For SYPRO Ruby staining, the 1:5 through 1:40 dilutions were mixed 1:1 with 1X Laemmli Buffer (final) and Bicine/Chaps Lysis Buffer. Then, 3 µL of each sample were loaded on a 26-well 10% TGX gel and subjected to electrophoresis at 180 V for 40 minutes. Following electrophoresis, SYPRO Ruby staining was performed according to the manufacturer's basic protocol. Gel imaging was performed with ProteinSimple's FluorChem M, Software Version 4.1.1, with the settings below:

Step 1. Select "SYPRO Ruby"

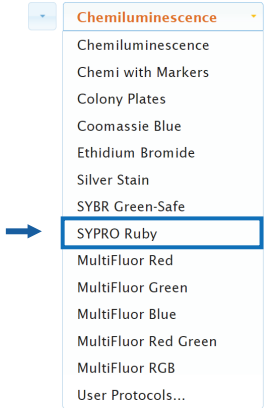

Step 2. Select "+ Add Channel"

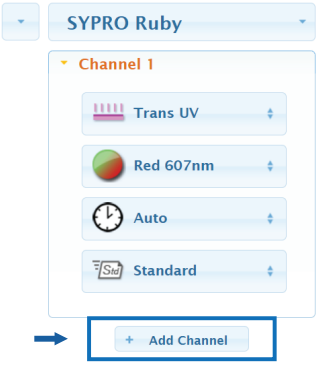

Step 3. Enter the settings below for the respective channels.

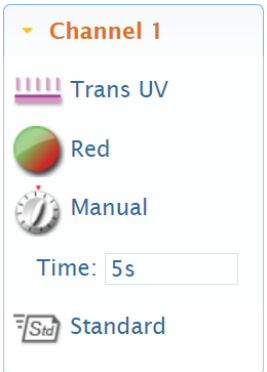

SYPRO Ruby Stain AAV Sample

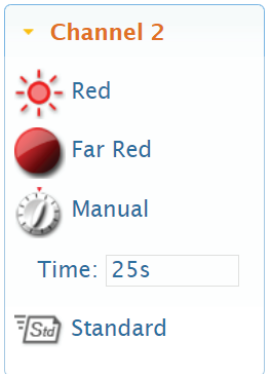

Precision Plus Dual Protein Standard Ladder

PUTTING THE 5X BIOTIN LABELING REAGENT TO THE TEST

To establish proof of concept, we compared 5X labeling reagent to 1X labeling reagent using a purified recombinant preparation of the molecular chaperone DnaK. DnaK was subjected to a 3-fold serial dilution series from 100 µg/mL to 0.123 µg/mL, and a 0 µg/mL concentration was included as a blank negative control. When this serial dilution series was analyzed on Jess using either 1X or 5X labeling reagent, the 5X labeling reagent resulted in a signal that was approximately 4- to 5-fold larger than the signal generated by the 1X labeling reagent (FIGURE 21A-C).

As expected, the 0 µg/mL sample concentration did not result in signal above background. The theoretical limit of detection and limit of quantification were compared between 1X and 5X labeling reagents, revealing an improvement in both metrics when the 5X labeling reagent was used (FIGURE 21D). Because Simple Western assays require as little as 3 µL of sample, the LOD of 0.05 µg/mL corresponds to just 150 pg of protein, which is only a fraction of what is reportedly required for SYPRO Ruby.[1-2]

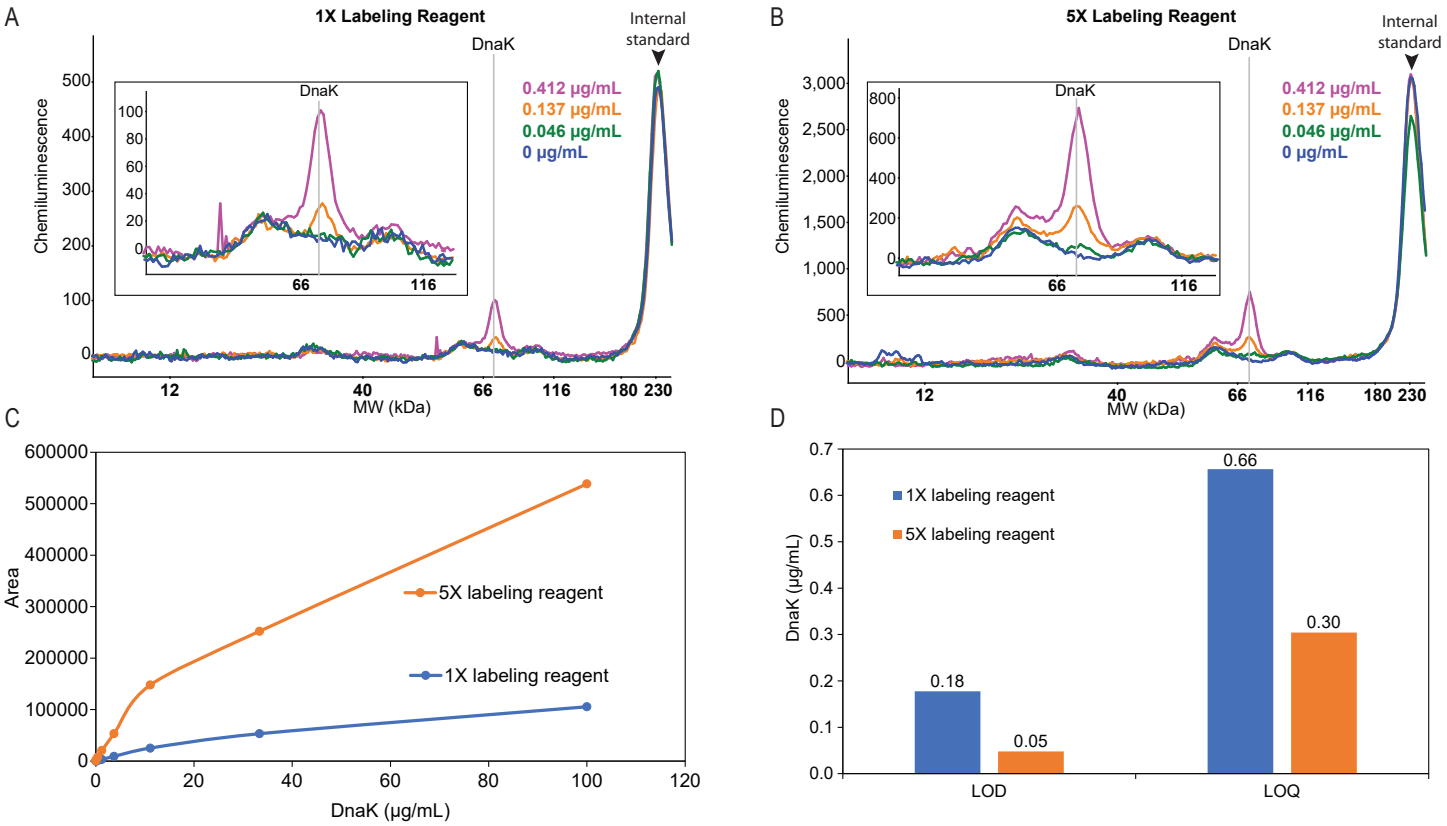

FIGURE 21. Labeling of DnaK with 5X labeling reagent increases assay signal 4- to 5-fold compared to 1X labeling reagent. Overlaid electropherograms of DnaK labeled with (**A**) 1X and (**B**) 5X labeling reagent. The insets are zoomed-in views of the DnaK signal. (**C**) Peak area by DnaK concentration and (**D**) LOD and LOQ determination of DnaK labeled with 1X and 5X labeling reagent.

APPLYING THE 5X LABELING REAGENT TO AAV ANALYSIS

Due to the tiny sample size requirements and enhanced sensitivity of this assay, it is particularly attractive for manufacturers of recombinant AAVs for gene therapy, which are difficult to manufacture and sample sizes are limiting. To mimic a real-world example, RNase A was spiked into a purified AAVs sample and analyzed with 1X and 5X total protein labeling reagent on Jess. The RNase A was serially diluted from 10 µg/mL down to 0.123 µg/mL, and a 0 µg/mL concentration was included as a blank negative control, and the AAV sample was held at a constant 1:10 dilution. As expected, the three AAV capsid proteins, VP1, VP2 and VP3, were clearly detected along with a singular RNase A peak that decreased with decreasing RNase A concentration (**FIGURE 22**). Under these conditions, the assay sensitivity for detecting RNase A increased about 3-fold with 5X labeling reagent when compared to 1X labeling reagent.

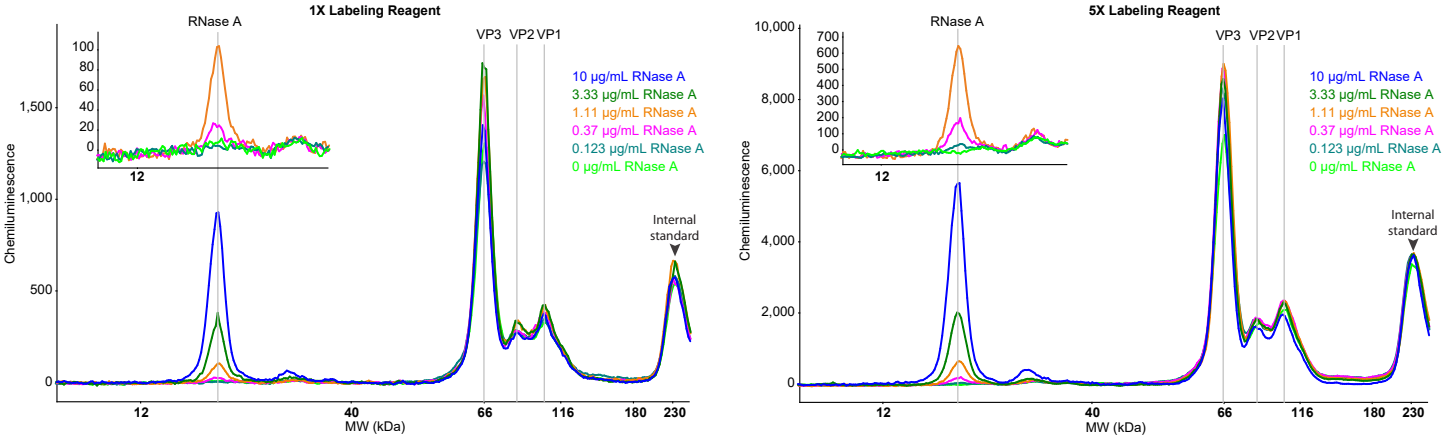

FIGURE 22. Overlaid electropherograms of AAV samples spiked with RNase A labeled with 1X (left) and 5X (right) labeling reagent. The insets are zoomed-in views of the RNase A signal.

MEASURING IDENTITY AND PURITY IN AAV SEROTYPES

A useful feature available on Simple Western systems is multiplex analysis by sequential immunoassays, known as RePlex™. It efficiently removes the antibodies from the first probing cycle for a second cycle of immunodetection without compromising assay robustness. The second probing round may be used to detect new targets, or it may be used for total protein normalization. Thus, we tested if 5X labeling reagent was compatible with the RePlex assay. In the first round, AAV capsid proteins were detected with anti-VP1 or anti-VP1/2/3 antibodies, and the second probing cycle was dedicated to total protein detection with 1X labeling reagent or 5X labeling reagent. The samples used in this analysis were crude, in-process samples and therefore a complex total protein profile is expected. From this analysis, the 5X labeling resulted in a ~5X increase in signal over the 1X label (**FIGURE 23**). While AAV1 and AAV4 did not have strong immunoreactivity with the anti-VP1/2/3 antibody, they did have similar total protein signals compared to AAV7 and AAV9 samples that do have strong immunoreactivity. This is expected as each sample was loaded at the same concentration of ~5 x 10^7 GC/mL. Taken together, these observations demonstrate that 5X labeling reagent is compatible for use in total protein normalization in RePlex assays.

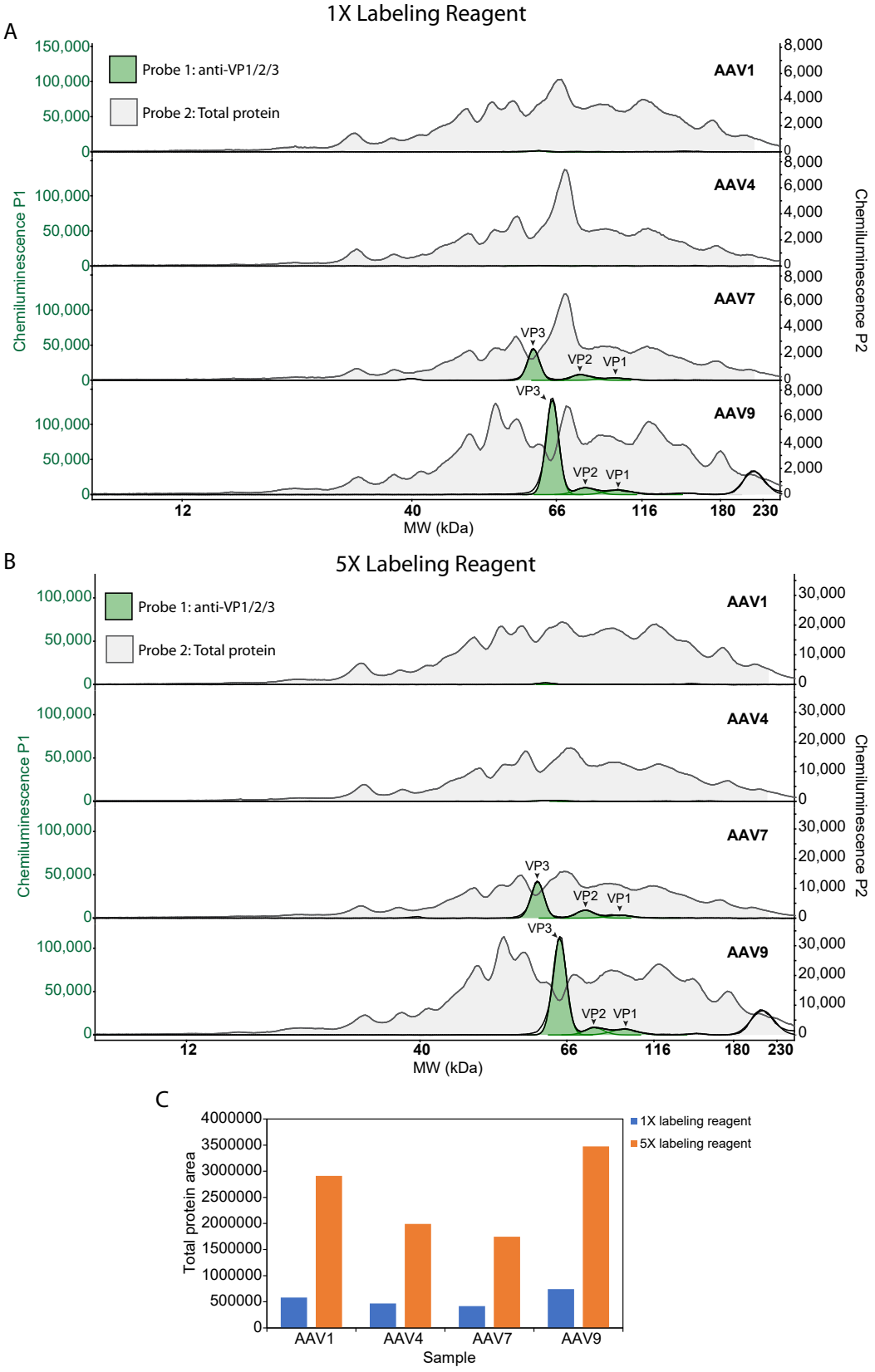

FIGURE 23. AAV immunoassay analysis with RePlex on Jess. Overlaid electropherograms of VP1/2/3 protein detection with the anti-VP1/2/3 antibody in the first probing cycle (green peaks) and total protein detection in the second probing cycle (gray peaks) with (**A**) 1X and (**B**) 5X biotin labeling reagent. All AAV samples were diluted 1:20 for a final concentration of 5 x 10^7 GC/mL. (**C**) Total protein area resulting from the second round of total protein detection with 1X and 5X labeling reagent.

SIMPLE WESTERN IS MORE SENSITIVE THAN SYPRO RUBY STAINING

SYPRO Ruby is among the most sensitive gel staining techniques, and many manufacturers of AAVs still rely on traditional SDS-PAGE with SYPRO Ruby staining to monitor purification. Unlike Simple Western, SYPRO Ruby staining is labor-intensive with many manual washing steps, generates large volumes of liquid waste, and requires special imaging equipment. Since AAV manufacturers could greatly benefit from replacing SYPRO Ruby staining with the automated Simple Western platform, we compared the sensitivity of the 5X labeling reagent on Wes with SYPRO Ruby staining by SDS-PAGE. To do so, we prepared AAV2 as described in the Materials and Methods and loaded equal volumes on SDS-PAGE with SYPRO Ruby staining and Wes with the 5X labeling reagent.

As expected, three signals corresponding to VP1, VP2, and VP3 appeared in both the SYPRO Ruby stain (**FIGURE 24A**) and by Wes analysis (**FIGURE 24B**). However, at the 1:40 dilution, the VP1 and VP2 peaks were hardly discernible above background levels on SYPRO Ruby staining (**FIGURE 24C**, right panel). On Wes, VP1 and VP2 peaks were clearly visible above background levels at the 1:40 dilution (**FIGURE 24C**, left panel). Furthermore, when peak area was plotted against sample dilution, a strong linear relationship was revealed on Wes, with $R^2 = 0.9992$, and the 1:40 dilution is within this linear dynamic range (**FIGURE 24B**, right panel). These results demonstrate that Simple Western analysis with 5X labeling reagent is more sensitive than SYPRO Ruby for the analysis of this AAV sample. In sum, Simple Western outperforms SYPRO Ruby in sensitivity in addition to improved automation and time to results.

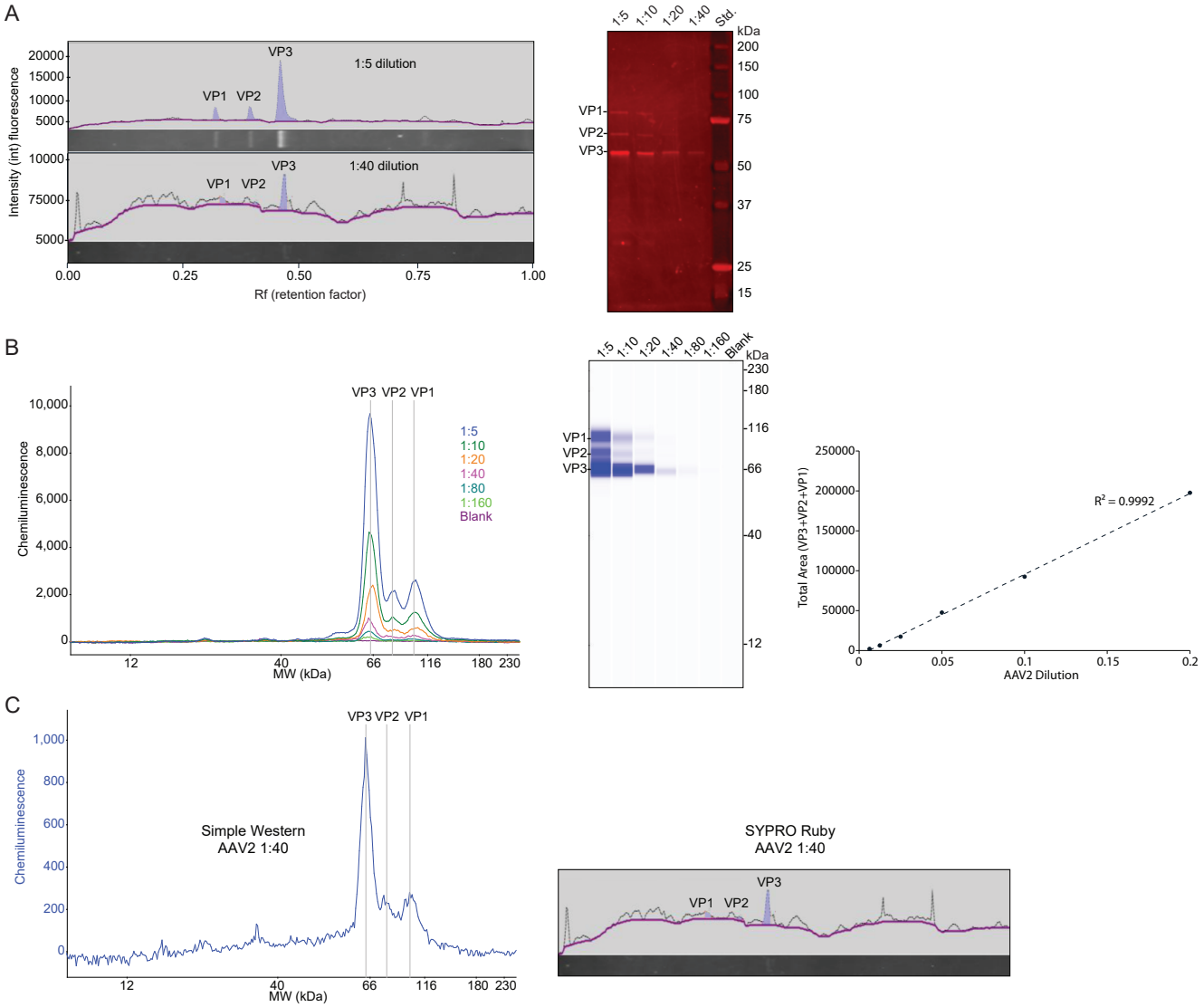

FIGURE 24. Comparison of AAV total protein detection with SYPRO Ruby and 5X labeling reagent with Wes. (**A**) SDS-PAGE stained with SYPRO Ruby (right) and densitometry analysis of the SYPRO Ruby stain (left); (**B**) Simple Western analysis graph view (left), lane view (middle), and linearity analysis (right); (**C**) Side-by-side comparison of the 1:40 dilution on Wes (left) and SYPRO Ruby (right).

LEADING SENSITIVITY COMBINED WITH SPEED AND AUTOMATION

With 5X biotin labeling reagent, Simple Western can achieve limits of detection in the upper picogram range. This is as good if not better than the best gel staining techniques like SYPRO Ruby and silver stain, which reportedly require lower nanogram levels for reliable detection.[3] Unlike messy gels, the Simple Western assay eliminates the hazardous waste generated by silver stain as well as all of the manual washing steps, with automated total protein detection in as little as 3 hours. And when it comes to AAV analysis, the use of 5X biotin labeling reagent gave results that were more sensitive than SYPRO Ruby. This is a major advantage for gene therapy because AAVs are difficult to manufacture and samples are extremely limiting. Also, the total protein concentration of AAV samples is often significantly lower than other biological therapeutics such as monoclonal antibodies. Therefore, a lower LOD may be required for AAV protein analytics. Finally, 5X total protein labeling reagent is compatible for use in RePlex, allowing users to get the most data out of their precious samples and normalize their protein expression data with confidence.

REFERENCES

1. Background-free, high sensitivity staining of proteins in one- and two-dimensional sodium dodecyl sulfate-polyacrylamide gels using a luminescent ruthenium complex, K. Berggren, E. Chernokalskaya, T. Steinberg, C. Kemper, M. Lopez, Z. Diwu, R. Haugland, and W. Patton, *Electrophoresis*, 2000; **21**:2509-2521.

2. A comparison between SYPRO Ruby and ruthenium II tris (bathophenanthroline disulfonate) as fluorescent stains for protein detection in gels, T. Rabilloud, J.M. Strub, S. Luche, A. van Dorsselaer, J. Lunardi, *Proteomics*, 2001; **1**:699-699.

3. A comparison of silver stain and SYPRO Ruby Protein Gel Stain with respect to protein detection in two-dimensional gels and identification by peptide mass profiling, M. Lopez, K. Berggren, E. Chernokalskaya, A. Lazarev, M. Robinson, and W. Patton, *Electrophoresis*, 2000; **21**:3673–3683.

Simple Western
Learn more | proteinsimple.com/simple_western_overview.html
Request pricing | proteinsimple.com/quote-request-simple-western-systems.html

Buy now | Total Protein Detection Module

CHAPTER 5: CHARACTERIZING CAR T-CELL THERAPY BIOMARKERS THROUGH MULTIANALYTE ANALYSIS

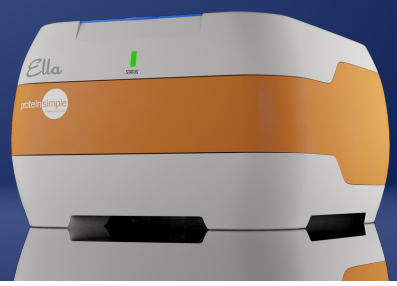

N.Steere, P. Younge, R. Weller Roska, M. Davila, M. Anderson | Bio-Techne, 614 McKinley Place NE, Minneapolis, MN 55413, *Moffitt Cancer Center 12902 USF Magnolia Drive # 12553, Tampa, FL 33612*

INTRODUCTION

Identification and monitoring of biomarkers related to T cell activation and associated cytokine release syndrome (CRS) will be necessary to fully realize the immense potential of chimeric antigen receptor (CAR) T-cell therapy. Such biomarkers could be used to guide clinical development of candidate therapies[1], provide mechanistic insight into patterns of resistance[2], and evaluate strategies to mitigate toxicity[3]. Establishment of predictive biomarkers is critical to maximizing therapeutic benefits of immunotherapy[4]. Correlating biomarkers with clinical evidence will facilitate early identification of patients at risk of developing CRS and enhance efforts to safely deliver CAR T therapy[5].

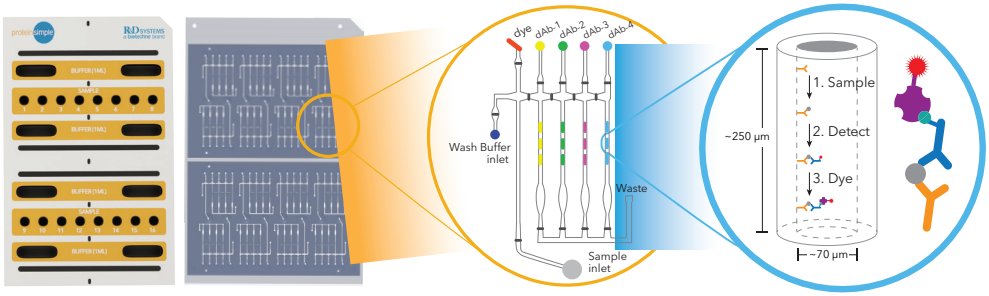

FIGURE 25. The Inner Workings of a Simple Plex Cartridge. Each sample well corresponds to a pneumatically-controlled microfluidic circuit, which contains 3 glass nanoreactors (GNRs) for each of 4 different analytes, along with all other necessary assay components. The inner diameter of each GNR contains analyte-specific capture antibody, while the remaining assay components are delivered pneumatically.

The successful identification of biomarkers to achieve these goals will require assays that meet several criteria. The assay must be able to simultaneously measure a broad panel of analytes with a high degree of accuracy within a brief timeframe[1,6], and provide rapid and efficient evaluation of patient response[3].

The Ella immunoassay platform with Simple Plex™ multianalyte assays enable fast and accurate quantitation of analytes of interest and allow for the detailed analysis of an individual's response to T cell infusion. A large catalog of validated assays, and a small required sample size (25 µL) make this hands-free assay well-suited for characterizing dynamic molecular response. In order to assess the utility of Ella in this context, we analyzed samples from three CAR T infused donors (10 time points each collected over 13 days, including pre and post- treatment for each donor).

METHODS

Serum samples from three individuals were collected over the course of 10 timepoints before, during, and following CAR T-cell therapy. Investigators were blind to the medical information of these individuals. All samples were evaluated on the Ella multianalyte immunoassay platform for the following human biomarkers: Granzyme A, Granzyme B, IFN-γ, IL-6, IL-10, IL-15, IP-10, and TNF-**α**. Each sample was diluted according to specific kit instructions and mixed prior to assaying. Assay run time for each 4-analyte cartridge was approximately 1 hour. The concentrations of biomarkers in each sample were quantified by comparison to standard curves for each analyte, which were generated and pre-loaded onto each cartridge during manufacture. All data was obtained via triplicate results per biomarker per well.

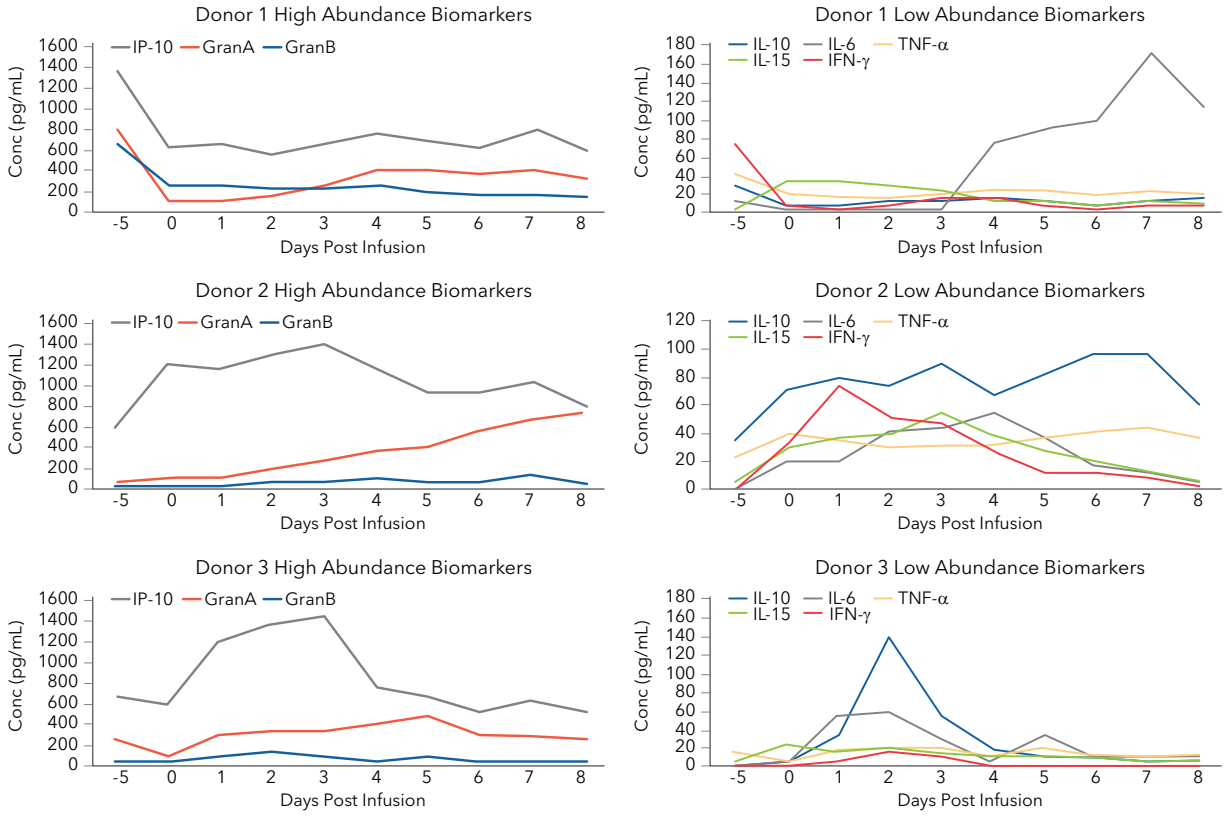

FIGURE 26. Each Donor Response Profile was Unique. Each donor presented a unique response profile. Elevated levels of many biomarkers were observed, with the degree of elevation and response time relative to T cell infusion varying between sample sets.

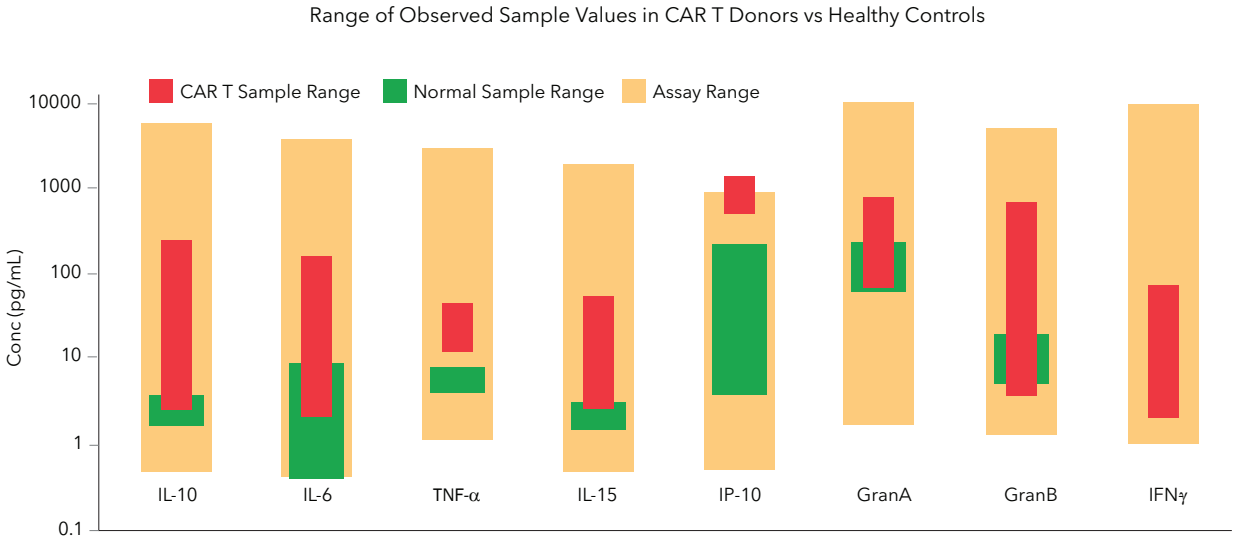

FIGURE 27. A Broad Range of Sample Values were Observed. The serum sample value range in the CAR T donor sample sets (n=3, 10 timepoints each) was broader than previously observed in healthy volunteers (n=10). The large dynamic range of the Simple Plex assays allowed for simultaneous quantitation of all analytes using a single dilution factor. Note that sample values shown here have been back calculated to account for dilution. IFN-γ levels in healthy controls were below the assay limits of quantitation.

DISCUSSION

As research investigating the clinical utility of CAR T-cell therapy continues, so too will the search for biomarkers which can be used to study subject response and assess potential risk. Our data, generated using Simple Plex immunoassay technology, shows biomarker response profiles varying considerably between donor sample sets (**FIGURE 26**). Donor 1 exhibited a uniquely elevated cytokine milieu prior to T cell infusion and showed little observable response until IL-6 increased drastically 4 days after infusion. By contrast, donors 2 and 3 exhibited increasing levels of IFN-γ, IL-6, IL-10, IL-15, and IP-10 within 24 hours of infusion. This heterogeneity of donor response, along with precipitous changes in cytokine abundance over short periods of time, highlight the importance of timely multianalyte analysis.

Collectively, the CAR T donor sample sets presented elevated levels for each biomarker compared to healthy controls. Sample value ranges were also broader in the CAR T donor sets compared to controls (**FIGURE 27**). The broad dynamic range of the Simple Plex assays allowed for quantitation of all biomarkers in all samples using a single dilution factor. Triplicate readings for each marker from every cartridge well, along with the pre-loaded standard curve provided confidence in the quality and continuity of our data. Characterizing CAR T-cell therapy biomarkers is a pursuit that demands robust, sensitive, and reproducible assays. In this context, the Ella instrument running Simple Plex Assays is an ideal platform.

REFERENCES

1. Biomarkers in T-cell therapy clinical trials, S.F. Lacey and M. Kalos, *Cytotherapy*, 2013; **5**:632.

2. Cancer immunotherapy trials underutilize immune response monitoring, C.M. Connell, et al., *The Oncologist*, 2018, **23**:116.

3. Kinetics and biomarkers of severe cytokine release syndrome after CD19 chimeric antigen receptor–modified T-cell therapy K.A. Hay, et al., *Blood*, 2017; **130**:2295.

4. Progress and challenges of predictive biomarkers of anti PD-1/PD-L1 immunotherapy: A systematic review, F. Teng, et al., *Cancer Letters*, 2018; 414:166.

5. Endothelial activation and blood–brain barrier disruption in neurotoxicity after adoptive immunotherapy with CD19 CAR-T cells, J. Gust, et al., *Cancer Discovery*, 2017; **7**:1.

6. Current concepts in the diagnosis and management of cytokine release syndrome, D. Lee, et al., *Blood*, 2014; **124**:188.

Learn more | proteinsimple.com/ella.html
Request price | proteinsimple.com/quote-request-simple-plex-system.html

CHAPTER 6: DETERMINING RESIDUAL BEAD COUNT: APPLICATION OF MICRO-FLOW IMAGING TO CAR T-CELL MANUFACTURING

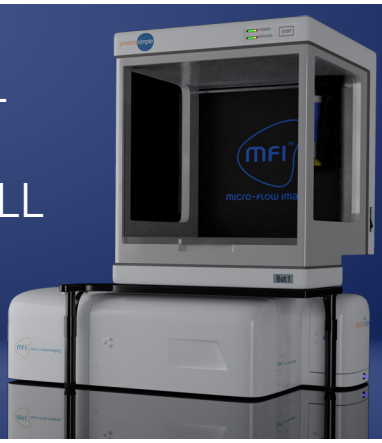

INTRODUCTION

Immunotherapy revs up the body's own natural defenses to fight cancer, veering away from traditional strategies that have, instead, focused on targeting the tumor and tumor cells. All of the enacting immunotherapeutic approaches incite hope, but especially those that uniquely engineer T cells to seek and destroy tumor cells. Chimeric antigen receptor (CAR) T-cell therapies, in particular, have produced booming immune responses and striking clinical outcomes with two such therapies already on the market and 800 clinical trials underway[1].

CAR T-cell therapy involves first isolating the patient's T cells and genetically modifying them to express a CAR on their surface capable of recognizing tumor-associated antigen(s). The engineered cells are then expanded ex vivo to an appropriate therapeutic dose and reinfused into the patient to stimulate an effective T-cell mediated anti-tumor immune response. From a manufacturing perspective, generating personalized batches of inherently complex CAR T-cell products poses real challenges for the biopharmaceutical industry. Regulatory agencies mandate that identity, purity, potency and safety attributes are closely monitored both in-process and for release. Of the process-related factors affecting product purity, residual beads during *ex vivo* expansion and activation of T cells pose safety and efficacy concerns with regard to triggering an unwanted endogenous immune response *in vivo*. Thus, compulsory limits are often set for residual bead counts to demonstrate product quality[2].

Residual bead count is typically determined manually by the naked eye and microscopy. But this approach is highly limited in its ability to accurately discern beads from cells and other potential in-process impurities, resulting in reporting uncertainties that risk regulatory approval. In this chapter, you'll see how automation via image-based Micro-Flow Imaging™ (MFI) technology gets you the quantitative and morphological data you need to have confidence in distinguishing between beads, T cells or other potential contaminants.

HOW DOES MFI WORK AND WHY USE IT FOR EVALUATING RESIDUAL BEADS DURING CAR T-CELL MANUFACTURING?

The MFI 5000 platform series uses flow-imaging technology to detect, quantify and characterize subvisible particles in as little as 600 µL of solution (**FIGURE 28**). The MFI 5200, specifically, can scrutinize particles in the 1 µm to 70 µm size range, making it the choice platform for distinguishing between particles like beads and lymphocytes. By collecting data across 10 different morphological parameters, MFI and the accompanying View System Software (MVSS) suite and MFI Image Analysis enable accurate and precise discrimination of particle populations in a 21 CFR Part 11 compliant workflow. In this instance, MFI's powerful software and filtering tools let you quickly and accurately measure polystyrene bead residual counts and other subvisible in-process contaminants that may have made their way into the final CAR T-cell product.

The C&GT field is evolving fast, making variability and the lack of defined processes a key challenge for manufacturers. When it comes to the residual bead count parameter of product purity, manual microscopy-based methods that rely on the human eye for reporting are employed—this is not only labor-intensive but also tough to scale and highly prone to error. Instead, the regulatory compliant MFI 5200 system can be applied to analyze mixed populations containing lingering

polystyrene beads among a high concentration of T cells. By adopting MFI, you'll get automatically quantified bead counts (even in low numbers), morphological data and, notably, a streamlined, reliable process for subset composition analysis.

MATERIALS AND METHODS

PREPARATION OF T-CELL SAMPLES AND ACTIVATION BEADS

For individual analysis, Dynabeads® Human T-Activator CD3/CD28 (ThermoFisher, PN 11161D) activation and expansion beads ($4x10^7$ beads/mL in PBS) were resuspended in 10X dilution series from 1:4 x 10^3 to 1:4 x 10^6 in 5 mL of PBS. Human Jurkat T lymphocyte cell samples were resuspended in the 10X dilution series from 1:25 to 1:2.5 x 10^5 in 5 mL of Cell Wash Buffer (20 mM Bicine, 250 mM Sucrose and 0.1% Kathon CG at a pH 7.5). For analysis of mixed populations, Jurkat cells were resuspended in the cell wash buffer to a final dilution of 1:250. Then, this solution was used as a diluent to resuspend Dynabeads in a 10X dilution series from 1:4 x 10^3 to 1:4 x 10^6 in 5 mL of cell wash buffer diluent, maintaining a constant dilution of cells.

SAMPLE RUNNING AND DATA ANALYSIS USING MFI 5200

Each sample dilution was analyzed in triplicate on the MFI 5200 series equipped with a 100 µm SP3 flow cell. The volume dispensed was 0.9 mL; the volume analyzed was 0.6 mL.

The Dynabeads utilized herein are precoated with anti-CD3 and anti-CD28 antibodies and are commonly used for ex vivo T-cell research applications, as they consistently supply the necessary primary and co-stimulatory signals that T cells need for activation and expansion. However, their micromagnetic nature also means they require additional steps and technologies to enable their removal—especially important for CAR T-cell therapies set to be infused into patients. The reality is, residual beads may remain, and you need a reliable and industry-compliant systems approach to accurately assess particle populations that affect product purity and, therefore, your regulatory filing. To demonstrate the power of MFI in discriminating and quantifying Dynabeads from a mixed population of cells–even in low numbers–we'll walk you through proof-of-concept examples and then show you how you can use MFI Image Analysis Software to further customize your parameters of interest.

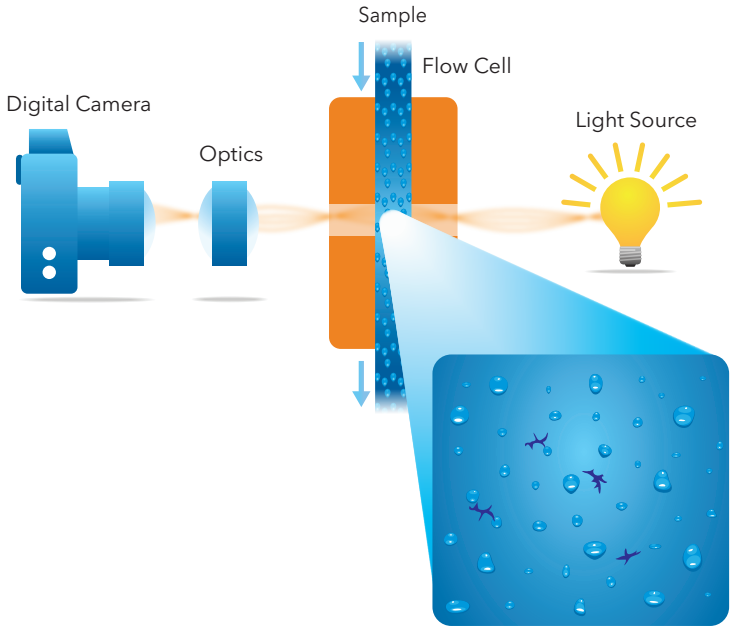

FIGURE 28. MFI technology principle. MFI uses a flow cell and digital optics to directly image, characterize and quantify subvisible particles in a liquid sample. The combination of digital microscopy and precise microfluidics gets you high-resolution images with 85% sampling efficiency. What's more, you'll get accurate counts and sizing information with full morphological detail for all subvisible particles in your sample.

SETTING THE STAGE FOR SUCCESS: SIZE, COUNT, REPEAT

Let's establish some essential characteristics of the two types of particles we're working with here: Jurkat T cells versus Dynabeads. In **FIGURE 29**, we took a 0.9 mL sample of Jurkat T cells or Dynabeads and ran each through an MFI 5200 series to collect morphological data. An average equivalent circular diameter (ECD) of 8.29 ± 1.85 µm for the T cells (expected size is 11.5 µm) and a 4.66 ± 0.66 µm ECD for Dynabeads (advertised diameter is 4.5 µm) was identified. Overall, a clear difference is seen when looking at the optical and morphological properties of each population on MFI. But how sensitive and reproducible is MFI for the distinction and quantification of such particles?

How well a technique reproduces the same result is at the crux of comparative intra- and inter-lab analyses. Variations in results using the same sample in the same laboratory may result in indeterminate conclusions or, worse, false reporting. In addition to being frustrating for analysts, irreproducible results incur added cost to the development process and negatively impact overall operations. So, the power of MFI in minimizing inconsistencies and maintaining reproducibility is easy to appreciate! To evaluate the sensitivity and reproducibility of MFI, we created a ten-fold dilution series of Jurkat T cells (**FIGURE 30**) and Dynabeads (**FIGURE 31**) for analysis. The bar graph in **FIGURE 30, left** shows overall equal and highly reproducible cell counts between runs and across the Jurkat T-cell replicate samples analyzed—detecting as little as five cells per milliliter. Attesting to the reproducibility of the system is the linearity of assay detection data (**FIGURE 30, right**), which measures the dilution factor versus the observed cell count from **FIGURE 30**, **left**, where a robust coefficient of determination (R^2) was achieved (≥0.99). Similarly, for Dynabeads (**FIGURE 31**), reproducible particle counts were observed across the dilution spectrum, counting as low as 5–10 beads/mL (**FIGURE 31, left**) with a robust R^2 value (≥0.99) (**FIGURE 31, right**). Taken together, these data are proof-of-concept of MFI's ability to accurately assess particle and/or cell counts in a sample.

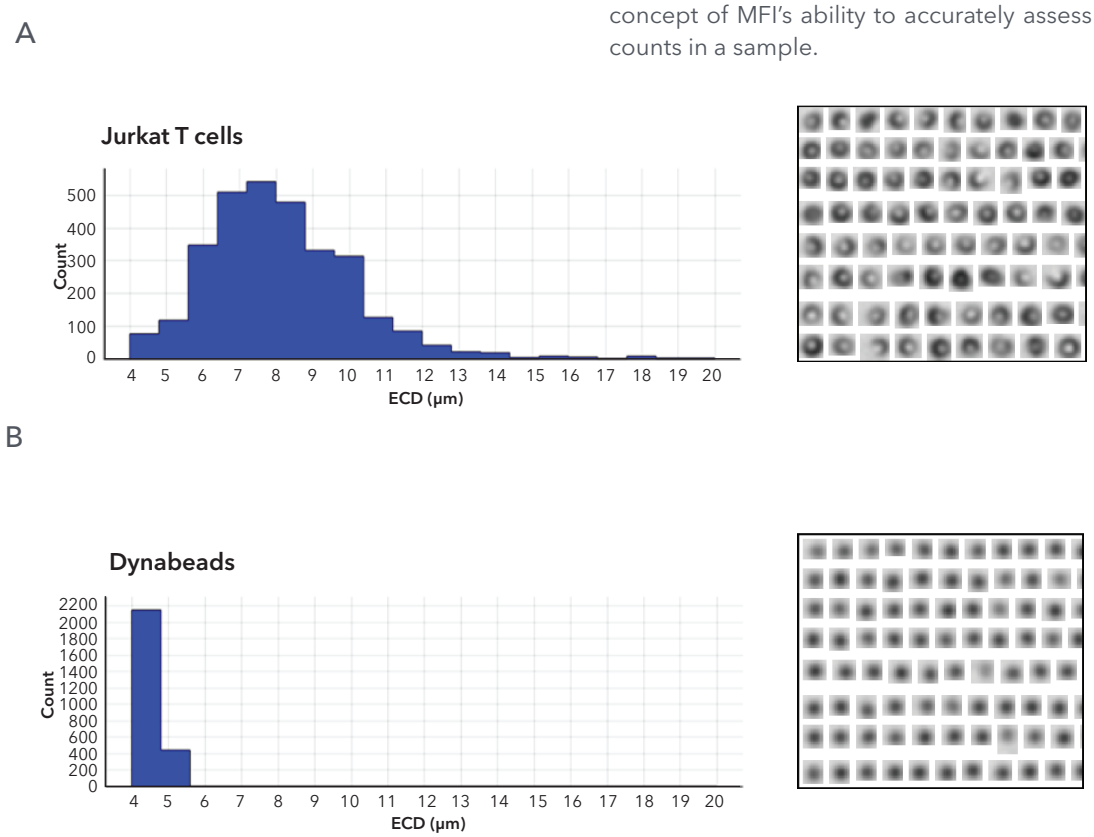

FIGURE 29. Particle size determination using MFI 5200. ECD measurements, which correlate to particle size, were automatically determined using MFI Image Analysis software for T cells (**A, left**) and Dynabeads (**B, left**). Each histogram shows the distribution of ECD in the two different particle types. Images of T cells (**A, right**) and Dynabeads (**B, right**) show distinct morphological features.

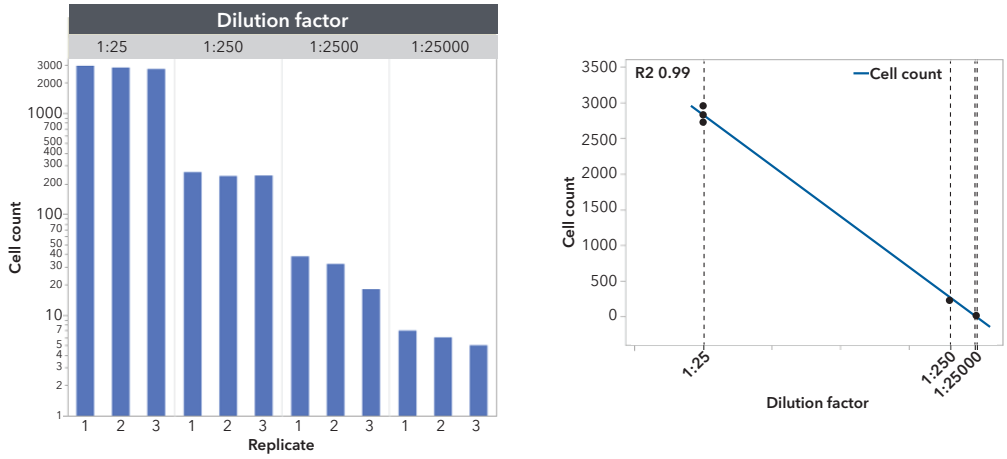

FIGURE 30. Quantitative reproducibility of MFI for the detection of Jurkat T cells. The observed cell count for the Jurkat T-cell dilution series analyzed in triplicate shows a linear decrease corresponding to the dilution factor that is reproducible with each replicate analyzed (**left**). The detection sensitivity was determined to be ~5 cells/mL. The linearity of this detection data (**right**) produced a robust R^2 value of ≥0.99

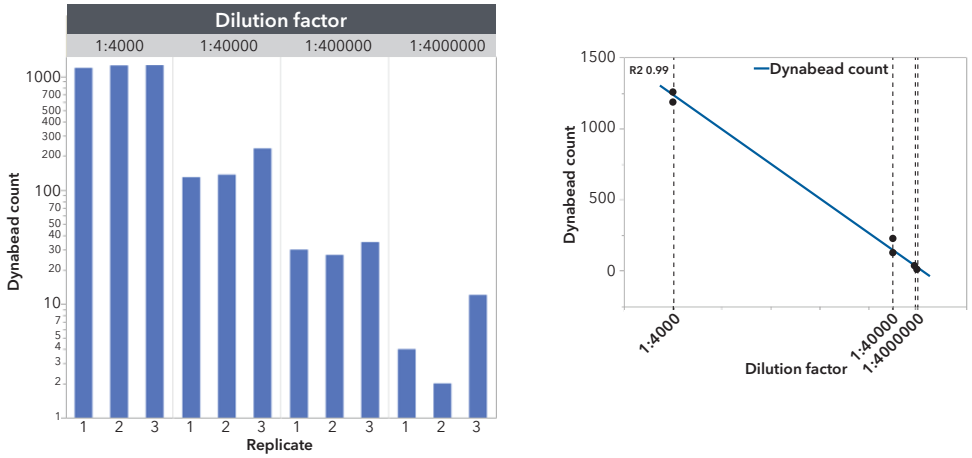

FIGURE 31. Quantitative reproducibility of MFI for the detection of Dynabeads. The observed bead count for the sample dilution series analyzed in triplicate shows a linear decrease corresponding to the dilution factor that is reproducible with each replicate analyzed (**left**). The detection sensitivity was determined to be 5–10 beads/mL. The linearity of this detection data (**right**) produced a robust R^2 value of ≥0.99.

BEYOND SIZE AND COUNT: DISTINGUISHING BETWEEN CELLS AND BEADS IN THE SAME SAMPLE USING MFI IMAGE ANALYSIS SOFTWARE

After data acquisition, you can use MFI Image Analysis Software to intuitively design filters and distinguish between particles based on 10 different morphological parameters! In FIGURE 32, we demonstrate this capability for Jurkat T-cell and Dynabead samples. Dynabeads have a well-defined ECD of 4.66 ± 0.66 µm, whereas lymphocyte ECDs can range from about 6 µM to 15 µM depending on the type and activation status[3,4]. This size difference was used as a basis for building appropriate filters that would discriminate between the two population types, in combination with circularity and intensity standard deviation measurements (FIGURE 32, **top and middle panels**). These parameters are not exhaustive, and filters in MFI Image Analysis Software may be tailored for any particle type. For example, layers can be added or removed, and parameter limits can be tuned for each filter. A complete list of available customizable parameters is also displayed in FIGURE 32, **bottom panel**.

Filters: T cells

Name	Property	Test	Level	Count	Concentration (#/ml)	Population (%)
All	Remove Stuck, Slow			5538	9070.13	98.84
Filter 1	ECD	>=	5.0	514	841.83	9.17
Filter 2	ECD	<=	15.0	514	841.83	9.17
Filter 3	Circularity	>	0.3	514	841.83	9.17
Filter 4	Intensity Std	>=	60.0	508	832.00	9.07
Filter 5	Intensity Std	<=	250.0	508	832.00	9.07

Filters: Dynabeads

Name	Property	Test	Level	Count	Concentration (#/ml)	Population (%)
All	Remove Stuck, Slow			5538	9070.13	98.84
Filter 1	ECD	>=	3.0	5199	8514.91	92.79
Filter 2	ECD	<=	5.0	4685	7673.09	83.62
Filter 3	Circularity	>	0.7	4680	7664.90	83.53
Filter 4	Intensity Std	>=	100.0	4662	7635.42	83.21
Filter 5	Intensity Std	<=	200.0	4662	7635.42	83.21

FILTERS AVAILABLE IN MFI IMAGE ANALYSIS SOFTWARE

- Equivalent circular diameter (ECD)
- Area
- Perimeter
- Circularity
- Aspect ratio
- Max Feret diameter
- X position
- Intensity mean
- Intensity standard deviation
- Intensity minimum
- Intensity maximum
- Time (%)
- Time (minutes)

FIGURE 32. Customizing filters using MFI Image Analysis Software. Presetting your own filters allows for the particle subpopulations present to be automatically filtered. Filter settings for Jurkat T cells (top panel); Dynabeads (middle panel) and a complete list of available filters (bottom panel) are shown. ECD, equivalent circular diameter; Circularity, the circumference of a circle with an equivalent area divided by the actual perimeter of the particle; Intensity Std, the standard deviation of the intensity of all pixels representing the particle.

Previously, we analyzed Dynabeads and Jurkat T cells as individual samples. Now, in **FIGURE 33**, we demonstrate that MFI can parse the two populations, even from a mixed sample. The filter customization in **FIGURE 33**, which shows that circularity and intensity standard deviation are additional layers to the base layer of ECD, more precisely define each population in this sample based on their properties. Because ECD is the base property for these two filters, it is shown in **FIGURE 33** to represent the two populations of particles.

In a real-world example, Dynabeads are often used for cell selection and activation without the need for removal until harvest. As such, residual bead count checks are critical and commonly performed once the appropriate therapeutic CAR T-cell dose is achieved, and you're ready for product lot release. To examine whether MFI could reproducibly count even small numbers of Dynabeads in the presence of a constant number of cells, we prepared a dilution series of Dynabeads while maintaining a constant dilution of Jurkat T cells (1:250). **FIGURE 34** represents these analyses, where MFI was able to reproducibly and accurately identify as few as 10 Dynabeads in a cell solution!

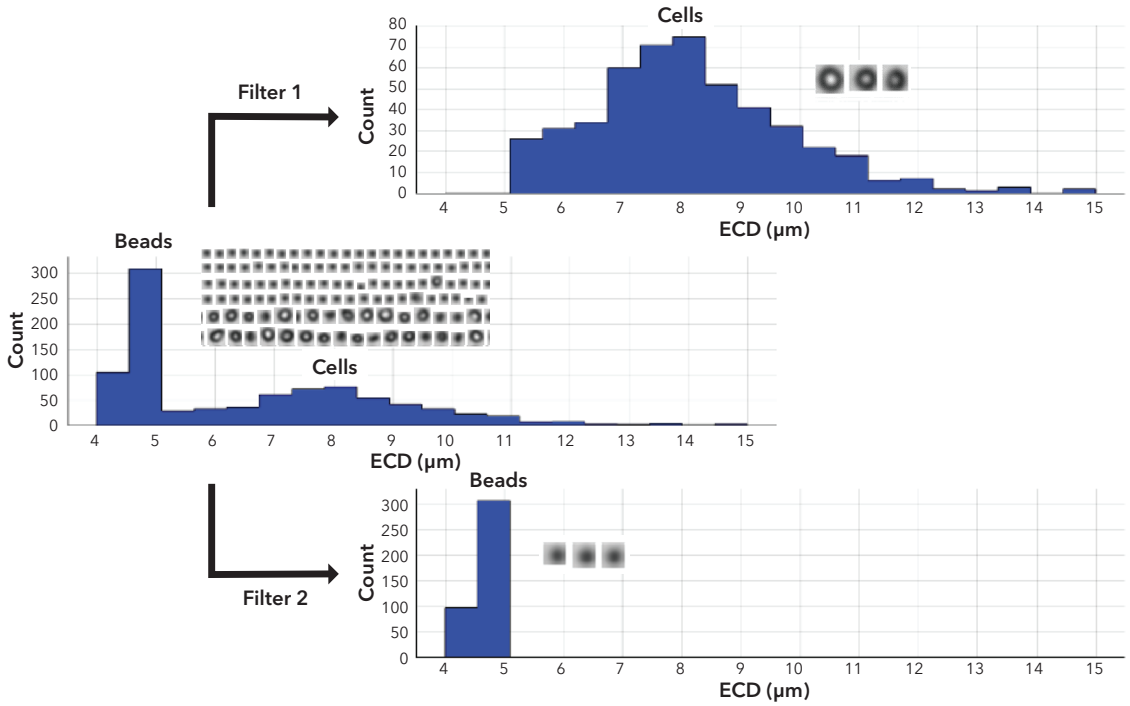

FIGURE 33. MFI can distinguish beads from cells in a mixed population.

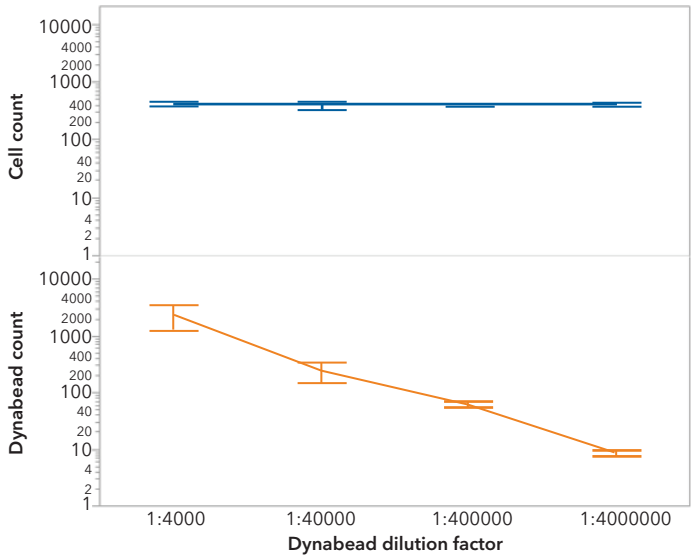

FIGURE 34. MFI can identify and count small numbers of Dynabeads in the presence of T cells. The counting of beads was unaffected by the presence of cells. A linear decrease in Dynabead count with dilution factor was observed despite the presence of T cells, and a reproducible number of Dynabeads was counted for each dilution.

SAID AND DONE: CLEANING THE FLOW CELL

Subvisible particle detection and characterization via MFI is dependent on precise and accurate imaging of a solution as it passes through the flow cell. As such, this flow cell is treated with a hydrophobic silane coating to prevent particle adhesion, as proteins and particles can stick to its interfaces and surfaces. When working with biohazardous samples, a bleach solution is typically used to ensure all living materials and associated risks have been neutralized. To test the robustness of the flow cell silane coating, we tracked the percent of total particles that are either slow-moving or stuck after repeated cleanings (96 flushes at a rate of 6 mL/minute) with a 10% bleach solution (FIGURE 35).

Then, the system was evaluated with suspensions of the National Institute of Standards and Technology Certified Particle Size Standard, 5 µm (ProteinSimple, PN 4004-001-001), which was analyzed after every other bleach flush. The total particle count and the percent of slow-moving and non-recovered particles were calculated (FIGURE 35). No increase in the percent stuck or slow-moving particles were observed over the course of our testing period, indicating that the silane coating remained intact.

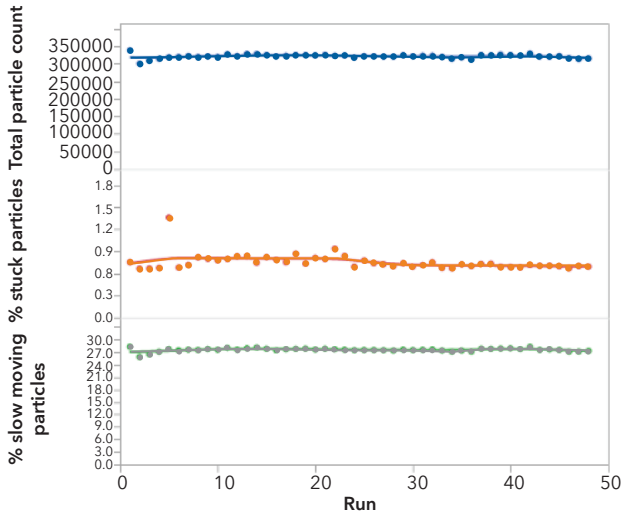

FIGURE 35. Particle count after MFI flow cell cleaning. The MFI flow cell was repeatedly cleaned with a 10% bleach solution, which did not affect the silane coating and all 48 subsequent runs tracking particle movement. The first data point corresponds to a run performed before bleach exposure, indicating no change in performance before and after bleach exposure.

CONCLUSION

Residual beads from in-process CAR T-cell manufacturing workflows may pose immunogenicity concerns and delay the release of your final product. Ensuring their removal is, therefore, an essential step to on-track regulatory approval. To confirm the product's purity, you'll need to accurately assess its composition for the presence of subvisible particles, including the reporting of residual bead count. Current approaches are not reliable or reproducible as they involve manual counting and rely on the human eye to discern between particle types and cells. But MFI is an image-based, automated system that gives you the advantage over compendial techniques for this type of analysis. By directly imaging particles and collecting morphological data, MFI enables the quantification and discrimination of T cells from activation beads in a mixed population. You'll also be able to detect even low numbers of beads within a large population of T cells, giving you more confidence in the vital decisions you make during development and manufacturing!

REFERENCES

1. The global pipeline of cell therapies for cancer, J.X. Yu, V.M. Hubbard-Lucey and J. Tang, *Nature Reviews Drug* Discovery, 2019, **18**; 821–822.

2. Standards and Best Practices for Cell, Gene and Tissue-based Therapies, R. Potts, U.S. Pharmacopeial Convention. Available online at cdn.ymaws.com/www.casss.org/resource/resmgr/cmc_no_am_jul_spkr_slds/2017_CMCS_PottsRebecca.pdf. Updated 18 July 2017. Accessed 8 January 2020.

3. Dynabeads® Human T-Activator CD3/CD28, ThermoFisher Instruction Manual. Available online at assets.thermofisher.com/TFS-Assets/LSG/manuals/11131D_32D_61D.pdf. Accessed 13 January 2020.

4. The Histology Guide, Faculty of Biological Sciences, University of Leeds. Available online at www.histology.leeds.ac.uk/

Learn more | proteinsimple.com/mfi_5000.html
Request price | proteinsimple.com/quote-request-micro-flow-imaging-systems.html

PIONEERING CELL & GENE THERAPY SOLUTIONS: FROM DISCOVERY TO THE CLINIC

Your vision is to create revolutionary C&GT to treat life-threatening diseases. Bio-Techne and its family of brands is on this journey with you. While the focus of this eBook is on analytical solutions to drive your C&GT research forward, Bio-Techne is a full-solution ancillary reagent and services provider. We will stand by you, providing flexible and pioneering tools to simplify your workflow. From CAR T-cells to pluripotent stem cells, let us help you get your therapy to the patients that need it!

For more information on additional solutions that Bio-Techne offers in C&GT, check out the resources below:

Cell separation and characterization | bio-techne.com/cgtseparation

Gene editing | rndsystems.com/services

GMP recombinant proteins | rndsystems.com/gmp

GMP small molecules | tocris.com/gmp

GMP cell culture reagents | bio-techne.com/cgtculture

Product release and testing | bio-techne.com/cgtquality